Analytic self-pulsing solutions and their instabilities in a homogeneously broadened ring laser

Hong Fu
Institut für Theoretische Physik und Synergetik, Universität Stuttgart, D-7000 Stuttgart 80, Federal Republic of Germany
(Received 26 January 1989)

Analytical traveling-wave self-pulsing solutions of a homogeneously broadened ring laser are presented in the limit that the dipole relaxation rate is much greater than the atomic inversion relaxation rate. The phase velocity $v(\Lambda)$ as a function of the normalized pump Λ is given explicitly. This function has a simple relation with the upper boundary $\alpha_{\max}(\Lambda)$ of the Risken-Nummedal-Graham-Haken (RNGH) instability domain in the (α,Λ) plane, where α is the wave vector of the perturbations. The self-pulsing may appear in different ways, depending on how the stationary solution becomes unstable. If the instability of the stationary solution is caused by an unstable mode touching upon the upper boundary of the RNGH-instability domain in the (α,Λ) plane, the self-pulsing is supercritical; if the unstable mode lies on the lower boundary, a subcritical self-pulsing arises, and the system is bistable. This rule provides new signatures of the self-pulsing phenomena and will be helpful to experimental identification of the self-pulsing arising from the RNGH instability. The linear stability analysis reveals two kinds of instabilities for these self-pulsing solutions. One kind of instability is rooted in the RNGH instability of the stationary solution and may occur even when the amplitude of the self-pulsing solution approaches zero. The other kind of instability occurs when the oscillating amplitude of the self-pulsing solution becomes large. Above this large-amplitude instability threshold no traveling-wave self-pulsing can be stable any longer. The results for the corresponding Lorenz model are also presented.

I. INTRODUCTION

The multimode instability in a homogeneously broadened unidirectional ring laser was first investigated by Risken and Nummedal[1] and Graham and Haken[2] in 1968. They found that the stationary solution in the on-resonance case experiences a multimode instability if the pumping reaches a critical value (see Secs. II A and III) and predicted the onset of ultrashort self-pulsing. This critical pumping is usually called the second threshold, in contrast to the first threshold, where lasing begins. Direct numerical integration of the Maxwell-Bloch laser equations showed that the steady self-pulsing solution is a traveling wave, and for certain values of the cavity length the pulsing solution can be stable below the second threshold.[1]

In the vicinity of the stability threshold, the self-pulsing was analyzed by Haken, and Haken and Ohno[3–6] as an extension of the Ginzburg-Landau theory of phase transitions to systems far from equilibrium,[7,8] and the results of the temporal form of the laser output were found to be in good agreement with the numerical solutions of Risken and Nummedal.

After the work of Haken in establishing the fundamental link between a single-mode laser and the Lorenz model,[9] Graham showed that a similar analogy exists between a phase-locked multimode laser and the Lorenz model.[10] By means of this analogy, he derived the second threshold in a way that connects it to the Lorenz instability.

By numerical integration Mayr, Risken, and Vollmer found that, for a still higher pump parameter, even the pulses themselves will change and either chaotic or periodic breathing of the pulse can occur.[11]

More recently, the treatment of the multimode instability in homogeneously broadened unidirectional ring lasers above the second threshold has been extended by many authors to consider different cases, and the results show that the multimode laser possesses a rather complicated phenomenology.[12–20] We will only mention some of them which are closely related to the Risken-Nummedal-Graham-Haken (RNGH) instability and are of interest for the present paper.

The first consideration of detuning in a homogeneously broadened multimode laser was provided by Zorell,[21] who investigated small detuning values and found that the *amplitude* eigenvalue was responsible for the onset of unstable behavior at a higher excitation level than in the corresponding resonant case. More recent studies by Narducci *et al.*[22] and Lugiato *et al.*,[23] have shown that, out of resonance, the *phase* eigenvalue can become responsible for the development of an instability. Therefore the instability is brought about by a destabilization of the phase, that is, by a mechanism that is different from the one that is operative in connection with the RNGH instability.

Also significant is the work of Lugiato *et al.*[24] in which they generalized the earlier treatment of Risken and Nummedal[1] and Graham and Haken[2] to allow arbitrary values for the ring-cavity transmission, so that the longitudinal profile of the stationary field and of the atomic variables is no longer a constant. In addition to the self-pulsing phenomena, the injection of numerical

noise shows the presence of numerous coexisting basins of attraction for higher pump parameters.

Kotomtseva, Loiko, and Samson have proposed a mathematical model for investigating instabilities of various layer systems.[25,26] Based on this model, the physical processes creating instabilities in a standing-wave laser are classified. Possible successions of bifurcations are identified, which switch the system from stationary solution to periodic, quasiperiodic, and irregular self-pulsing regimes in the laser.

It is worth mentioning the experimental observations of the higher-order instabilities and multichromatic operations in dye lasers by Hillman *et al.*,[27] Stroud, Koch, and Chakmakjian,[28,29] and Lawandy, Afzal, and Rabinovich.[30] These new experimental phenomena have addressed the question of multimode instabilities in homogeneously broadened systems and have inspired many theoretical investigations.[24,27,30–36] We believe that the multichromatic operations and the higher-order instabilities are rooted in the band structure of the energy level of dye molecules and are not directly related to the RNGH instability.[34–36]

We mention in passing that the self-pulsing phenomena in inhomogeneously broadened lasers have been extensively studied by Casperson[37] and other authors.[12–20]

Although much work has been devoted to the investigation of self-pulsing in homogeneously broadened lasers, it has still remained one of the more poorly understood phenomena, at least in the following aspects.

Though numerical integrations reveal that the self-pulsing is a traveling wave at pump not too far above the second threshold[1,24] (for review papers see Refs. 13, 15, 17, and 19), how the phase velocity of the pulse depends on the other parameters is unknown. This means that the Prandtl number in the corresponding Lorenz equations is undetermined.[10]

Though previous work demonstrates that both supercritical and subcritical self-pulsing may develop from the RNGH instability,[1,4–6,13,25,31] no simple rule has been found that tells whether the self-pulsing will be a supercritical or a subcritical one for a concrete system.

Though numerical investigations have shown that a self-pulsing may exist and may become unstable under certain conditions,[1,4–6,11,24–26] the linear stability analysis for the self-pulsing based on the full set of Maxwell-Bloch equations is still lacking.

The purpose of this paper is to present results with respect to these and some other aspects based on an analytically soluble model. This model is the usual two-level, homogeneously broadened, unidirectional ring laser in the resonant case[1–6,10,11,38,39] under the assumption that the dipole relaxation rate $\gamma_\perp$ is much greater than the atomic inversion relaxation rate $\gamma_\parallel$. In this limit, we are able to obtain analytical self-pulsing solutions in order to determine the phase velocity as a function of the pump, to find out the relations between the self-pulsing and the RNGH instability, and to analyze the linear stability of the self-pulsing solutions. All of these were considered to be a forbiddingly difficult task in the general case.

Since the work is based on the full set of the multimode Maxwell-Bloch laser equations,[38,39] i.e., we do not eliminate the polarization, our results not only apply to lasers satisfying $\gamma=\gamma_\parallel/\gamma_\perp \ll 1$, which include solid-state lasers, semiconductor lasers, dye lasers, and CO_2 lasers, but also provide insight into lasers with arbitrary γ.

It should be noted that our investigations are limited for traveling-wave pulsations. In this case, all the Fourier components of the pulsation are locked in frequency and the pulsation consists of just one basic frequency component apart from its harmonics. The physics of this mode locking is not quite clear (for mode locking of lasers see Ref. 12), even though the stability of the self-pulsing solution for pump not too far above the second threshold justifies the existence of such solutions.

The main results and the organization of the paper are as follows. The Maxwell-Bloch equations for a traveling-wave pulsation are analytically solved for the first time in Sec. II. The solutions are given in an explicit form with two variables to be determined, namely, the phase velocity and the number of the periods of the pulse appearing in the cavity, which will be called the pulse number in this paper. The phase velocity is determined by the periodicity of the laser cavity as a function of the pump parameter. It is shown analytically that the velocity is always greater than the velocity of light in the active medium, a result already suggested by numerical integrations,[1] and by analytical calculations in the vicinity of the second threshold.[4,6] In comparison to Ref. 31 this result means that the model used here permits only the *fast* (i.e., $v>c$) pulsations to occur, but not the *slow* (i.e., $v<c$) ones.

In Sec. III a relation between the self-pulsing solutions and the boundaries of the RNGH-instability domain in the (α,Λ) plane is established, where α and Λ are the wave vector and the pump, respectively. Based on this relation, we show that the pulse number is largely limited for a stable pulsing solution. Furthermore, we show that the pulsation may appear in different ways, depending on how the RNGH instability of the stationary solution occurs. If the unstable mode lies on the upper boundary, then a supercritical pulsation will appear above the RNGH threshold; if it lies on the lower boundary, a subcritical pulsation arises and the system is bistable.

The linear stability analysis of the self-pulsing solutions is performed in Sec. IV based on the full set of the Maxwell-Bloch equations.

In the good cavity limit, two Floquet exponents prove to be relevant to the stability of the self-pulsing. One of them may be calculated analytically and is shown to be nonpositive. The other one is analytically discussed in Sec. V in the small-amplitude limit and is numerically studied in Sec. VI.

The linear stability analysis reveals two kinds of instabilities for these pulsing solutions. One kind of the instabilities is rooted in the RNGH instability of the stationary solution and may occur even when the amplitude of the self-pulsing solution approaches zero. This instability will be called RNGH-type instability. The other kind of instabilities occurs when the oscillating amplitude of the self-pulsing solution becomes large. Above this large-amplitude instability threshold there is no stable

traveling-wave self-pulsing any more. Numerically it is known that different complicated solutions may exist,[11,24–26] but we do not know to which state the system would switch. It should be noted that both the RNGH-type instabilities and large-amplitude instabilities refer to the self-pulsing solutions, while the RNGH instability refers to the stationary solution.

In Sec. VII relations between the self-pulsing solutions and the Lorenz model are discussed. It is shown that the self-pulsing solutions are confined on one branch of the critical curve in the parametric plane expanded by the Prandtl number and Rayleigh number on which the Lorenz instability for the stationary solution sets in. The results and some open questions are discussed in Sec. VIII.

II. MAXWELL-BLOCH EQUATIONS AND THE SELF-PULSING SOLUTION

A. Maxwell-Bloch equations

The starting point for this study is the same set of Maxwell-Bloch equations[38–40] that was the basis for earlier studies of multimode instabilities in homogeneously broadened, unidirectional ring lasers:[1–6,10,11]

$$\frac{\partial E}{\partial t}+c\frac{\partial E}{\partial x}=\kappa(P-E) , \tag{1}$$

$$\frac{\partial P}{\partial t}=\gamma_{\perp}(ED-P) , \tag{2}$$

$$\frac{\partial D}{\partial t}=\gamma_{\parallel}\left[\Lambda+1-D-\frac{\Lambda}{2}(EP^*+E^*P)\right] , \tag{3}$$

where E refers to the electric field strength, P to the macroscopic polarization, and D to the macroscopic inversion density of the active medium, which have been normalized with respect to their steady-state values. κ, $\gamma_{\perp}$, and $\gamma_{\parallel}$ are the cavity loss, the relaxation rate of the polarization, and the relaxation of the atomic inversion, respectively. Λ is the pump parameter defined by $\Lambda\equiv(D_0-D_{\rm thr})/D_{\rm thr}$, where D_0 is the unsaturated macroscopic inversion density and $D_{\rm thr}$ the macroscopic inversion density at the lasing threshold. c is the velocity of light in the medium.

By definition, $\Lambda=0$ is the lasing threshold and for $\Lambda\geq 0$ there exists a stable time-independent solution. Stability analysis of these equations in the on-resonance case shows that this stationary solution experiences a multimode instability if Λ exceeds the second threshold.[1,2] In the present paper, we call this instability the RNGH instability and denote the second threshold by $\Lambda_{\rm RNGH}$. A short description of the RNGH instability and the determination of $\Lambda_{\rm RNGH}$ will be presented in Sec. III.

It is our purpose to study the space- and time-dependent solutions developing from this instability. Since the frequency of the unstable mode is of the order of $\sqrt{\gamma_{\parallel}\gamma_{\perp}}$, we normalize the space and time coordinates by

$$\tau\equiv\sqrt{\gamma_{\parallel}\gamma_{\perp}}t, \quad \zeta\equiv\sqrt{\gamma_{\parallel}\gamma_{\perp}}x . \tag{4}$$

In terms of the damping constants defined by

$$\chi\equiv\kappa/\gamma_{\perp}, \quad \gamma\equiv\gamma_{\parallel}/\gamma_{\perp} , \tag{5}$$

the Maxwell-Bloch equations (1)–(3) take the form

$$\sqrt{\gamma}\left[\frac{\partial E}{\partial\tau}+c\frac{\partial E}{\partial\zeta}\right]=\chi(P-E) , \tag{6}$$

$$\sqrt{\gamma}\frac{\partial P}{\partial\tau}=ED-P , \tag{7}$$

$$\frac{\partial D}{\partial\tau}=\sqrt{\gamma}\left[\Lambda+1-D-\frac{\Lambda}{2}(EP^*+E^*P)\right] . \tag{8}$$

This set of Maxwell-Bloch equations is more convenient in discussing a self-pulsing laser in the limit $\gamma\to 0$.

B. Equations for traveling waves

Like the earlier work,[1,4–6,10] we discuss the traveling-wave self-pulsing solutions, i.e., we assume that the self-pulsing solutions are functions of the local time variable

$$\xi\equiv\tau-\zeta/v , \tag{9}$$

where v is the space- and time-independent phase velocity.

The self-consistency of this assumption is proved by the existence and the linear stability of the traveling-wave solution with respect to the full set of the Maxwell-Bloch equations as we shall see in this and the following sections.

Now we introduce a space-time–independent constant

$$\eta\equiv\frac{1}{\chi}\left[1-\frac{c}{v}\right] . \tag{10}$$

Later on we shall show that η is independent of χ and always satisfies $0<\eta<1$. Therefore, the limit $\chi\to 0$ will lead to $v\to c$ but not to a divergent η.

In terms of η, Eqs. (6)–(8) for the traveling-wave self-pulsing have the form

$$\sqrt{\gamma}\eta\frac{dE}{d\xi}=P-E , \tag{11}$$

$$\sqrt{\gamma}\frac{dP}{d\xi}=ED-P , \tag{12}$$

$$\frac{dD}{d\xi}=\sqrt{\gamma}\left[\Lambda+1-D-\frac{\Lambda}{2}(EP^*+E^*P)\right] . \tag{13}$$

We shall solve these equations in the limit $\gamma\to 0$ in the following sections.

C. The dominant part of the self-pulsing solution

As suggested by Eqs. (11)–(13), we expand all the unknown quantities F with respect to $\sqrt{\gamma}$

$$F=F_0+F_1\sqrt{\gamma}+F_2\gamma+\cdots , \tag{14}$$

where F may be E, P, and D.

In general, we should also expand η according to Eq. (14). However, it is easy to see that up to the order γ, η_2 and higher-order expansions will not be involved in our

discussions; and in the order of $\sqrt{\gamma}$, we can show that, though η_1 cannot be determined, it is irrelevant to all the physical results that we shall describe. For example, up to order γ, η_1 does not change the periodicity of the dynamic quantities, which puts restriction on the dynamic solutions, nor does it contribute to the real part of the Floquet exponents, which concerns the linear stability of the solutions. Therefore, for the sake of simplicity, we assume $\eta_1=0$ and $\eta=\eta_0$ in further discussions. In fact, $\eta_1=0$ is also supported by the discussions in Sec. VII. Results and expressions which contain η_1 as a free parameter are presented in Appendix B.

Inserting the series in Eqs. (11)–(13), we find, to the zeroth order, that

$$E_0=P_0, \quad D_0=1 . \tag{15}$$

In the first order of $\sqrt{\gamma}$, Eqs. (11)–(13) are

$$\eta\frac{dE_0}{d\xi}=P_1-E_1 , \tag{16}$$

$$\frac{dP_0}{d\xi}=E_0D_1-(P_1-E_1) , \tag{17}$$

$$\frac{dD_1}{d\xi}=\Lambda(1-E_0E_0^*) . \tag{18}$$

Eliminating (P_1-E_1) by equating Eqs. (16) and (17), and considering Eq. (15), we obtain

$$\frac{dE_0}{d\xi}=\frac{E_0D_1}{1+\eta} . \tag{19}$$

Now let us introduce the intensity $I\equiv EE^*$, which can be expanded into γ series according to Eq. (14), and the coefficients are given by

$$I_0=E_0E_0^*, \quad I_1=E_0^*E_1+E_0E_1^*, \ldots . \tag{20}$$

In terms of I_0, Eqs. (19) and (18) can be written as

$$(1+\eta)\frac{dI_0}{d\xi}=2I_0D_1 , \tag{21}$$

$$\frac{dD_1}{d\xi}=\Lambda(1-I_0) . \tag{22}$$

This set of nonlinear equations determines I_0 and hence it describes the dominant part of the self-pulsing solutions the limit $\gamma\rightarrow 0$.

In order to find the solutions for I_0 and D_1, we divide Eq. (21) by Eq. (22) and obtain

$$(1+\eta)\frac{dI_0}{dD_1}=\frac{2I_0D_1}{\Lambda(1-I_0)} , \tag{23}$$

which yields the solution

$$(1+\eta)\Lambda[\ln I_0(\xi)-\ln I_0(0)+I_0(0)-I_0(\xi)] =D_1^2(\xi)-D_1^2(0) , \tag{24}$$

where $I_0(0)$ is the initial value of $I_0(\xi)$. For a traveling wave, we may choose, without loss of generality,

$$I_0(0)=I_{\min}\equiv\min_{\xi}[I_0(\xi)] , \tag{25}$$

which implies, due to Eq. (21), that

$$D_1(0)=0 , \tag{26}$$

provided that $I_{\min}\neq 0$. Under this initial condition, Eq. (24) becomes

$$D_1^2(\xi)=(1+\eta)\Lambda[\ln I_0(\xi)-\ln I_{\min}+I_{\min}-I_0(\xi)] , \tag{27}$$

which yields

$$D_1(\xi)=\pm\sqrt{(1+\eta)\Lambda[\ln I_0(\xi)-\ln I_{\min}+I_{\min}-I_0(\xi)]} . \tag{28}$$

This equation may be used to calculate the maximum intensity

$$I_{\max}\equiv\max_{\xi}[I_0(\xi)] . \tag{29}$$

In fact, a pulse must reach its maximum $I_{\max}$, at least a local one, somewhere; and at this point $D_1(\xi)$ is equal to zero due to Eq. (21). Considering Eq. (28), this means

$$\ln I_{\min}-I_{\min}=\ln I_{\max}-I_{\max} . \tag{30}$$

It is easy to prove that for any given $I_{\min}\leq 1$ (or $I_{\max}\geq 1$), Eq. (31) uniquely determines $I_{\max}$ (or $I_{\min}$) satisfying $I_{\max}\geq 1$ (or $I_{\min}\leq 1$). This uniqueness means that all the local maxima of the pulse are equal to each other and so are the minima.

The inequality

$$I_{\min}\leq 1\leq I_{\max} \tag{31}$$

is expected because we can show by integrating Eq. (22) within one period that the average value of $I_0(\xi)$ is equal to unity.

The sign of D_1 given by Eq. (28) is determined by Eq. (21), i.e., $D_1(\xi)<0$ when $I_0(\xi)$ evolves from $I_{\max}$ to $I_{\min}$, and $D_1(\xi)>0$ when $I_0(\xi)$ evolves from $I_{\min}$ to $I_{\max}$.

Defining

$$\tilde{\Lambda}\equiv\frac{\Lambda}{1+\eta} \tag{32}$$

and substituting Eq. (28) into Eq. (21), we obtain

$$d\xi=\pm\frac{1}{2\sqrt{\tilde{\Lambda}}}\frac{dI_0}{I_0\sqrt{\ln I_0-\ln I_{\min}+I_{\min}-I_0}} . \tag{33}$$

Between the two maxima adjacent to the initial minimum, the solution is

$$\xi=\pm\frac{1}{2\sqrt{\tilde{\Lambda}}}\int_{I_{\min}}^{I_0(\xi)}\frac{dy}{y\sqrt{\ln y-\ln I_{\min}+I_{\min}-y}} . \tag{34}$$

Since all the maxima are equal to each other, Eq. (34) defines a periodic function $I_0(\xi)$ for given $I_{\min}$ (or $I_{\max}$) and $\tilde{\Lambda}$, see Fig. 1. Let T be the period of the pulse; we have from Eq. (34)

$$T=\frac{1}{\sqrt{\tilde{\Lambda}}}\int_{I_{\min}}^{I_{\max}}\frac{dy}{y\sqrt{\ln y-\ln I_{\min}+I_{\min}-y}} . \tag{35}$$

By means of Eq. (30) it is easy to show that Eq. (35) can be simplified as

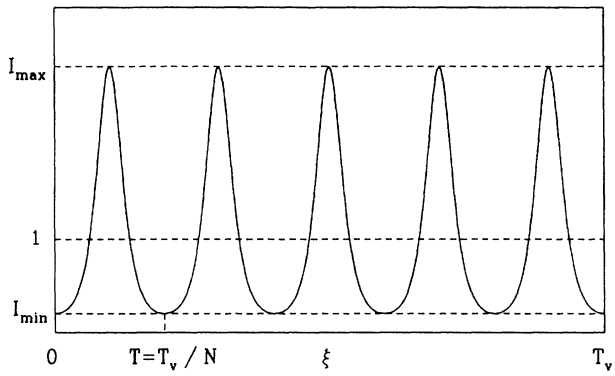

FIG. 1. Self-pulsing solution I_0 as a function of ξ in the case where there are $N=5$ pulses in the ring cavity.

$$T=\frac{1}{\sqrt{\tilde{\Lambda}}}\int_{I_{\min}}^{I_{\max}}\frac{dy}{\sqrt{\ln y-\ln I_{\min}+I_{\min}-y}} . \tag{36}$$

Notice that the period T of the pulse has to be compatible with the periodic ring boundary condition. Let L be the round-trip length of the ring cavity, then by the definitions Eqs. (4) and (9), the periodic boundary conditions takes the form

$$f(\xi)=f(\xi+L\sqrt{\gamma_{\parallel}\gamma_{\perp}}/v) . \tag{37}$$

In order to describe the periodicity of the self-pulsing solution with phase velocity v and the periodicity of the empty cavity, respectively, it is convenient to introduce

$$T_s\equiv\frac{L\sqrt{\gamma_{\parallel}\gamma_{\perp}}}{c},\quad T_v\equiv\frac{L\sqrt{\gamma_{\parallel}\gamma_{\perp}}}{v} , \tag{38}$$

which characterizes the periodicity of the system. Obviously, for the solution Eq. (36) to satisfy Eq. (37) it is necessary that

$$T=\frac{T_0}{N} , \tag{39}$$

where N is a natural number which describes how many pulses or peaks of the self-pulsing solution are in the laser cavity.

Combining Eqs. (36) and (39), we obtain a relation between $\tilde{\Lambda}$, $I_{\min}$, and T

$$T=\frac{1}{\sqrt{\tilde{\Lambda}}}\int_{I_{\min}}^{I_{\max}}\frac{dy}{\sqrt{\ln y-\ln I_{\min}+I_{\min}-y}} , \tag{40}$$

which can also be written in the form

$$\frac{c}{v}\sqrt{2\tilde{\Lambda}}=\frac{\sqrt{2}N}{T_s}\int_{I_{\min}}^{I_{\max}}\frac{dy}{\sqrt{\ln y-\ln I_{\min}+I_{\min}-y}} . \tag{41}$$

In Sec. II E, we shall show that η, and hence the left-hand side of Eq. (41), is a function of Λ. Therefore, for a given system parameters χ and T_s, we can calculate $I_{\min}$ of an N-pulse solution as a function of Λ from Eq. (41) and then solve the self-pulsing solution from Eq. (34).

D. The higher-order approximations of the self-pulsing solution

Though the higher-order approximations of the self-pulsing solution are negligible in the limit $\gamma\to 0$, we shall show that the periodicity of the solution of the order of γ requires η to be a function of Λ. In the order of γ, Eqs. (11)–(13) are

$$\eta\frac{dE_1}{d\xi}+\eta\frac{dE_0}{d\xi}=P_2-E_2 , \tag{42}$$

$$\frac{dP_1}{d\xi}=E_2-P_2+E_1D_1+E_0D_2 , \tag{43}$$

$$\frac{dD_2}{d\xi}=-D_1-\Lambda E_0(E_1+P_1) , \tag{44}$$

where $E_0=P_0$ and $D_0=1$ have been considered. From Eqs. (16) and (19), P_1 can be expressed by E_0 and D_1 as

$$P_1=\frac{\eta}{1+\eta}E_0D_1+E_1 . \tag{45}$$

Eliminating (P_2-E_2) from Eqs. (42) and (43) and taking Eq. (45) into account, we obtain the following equations for E_1 and D_2:

$$(1+\eta)\frac{dE_1}{d\xi}=E_1D_1+E_0D_2-\eta\frac{d^2E_0}{d\xi^2} , \tag{46}$$

$$\frac{dD_2}{d\xi}=-D_1-2\Lambda E_0E_1-\Lambda\eta E_0\frac{dE_0}{d\xi} . \tag{47}$$

Since

$$(1+\eta)E_0\frac{dE_1}{d\xi}=(1+\eta)\frac{d(E_0E_1)}{d\xi}-E_0E_1D_1 \tag{48}$$

and

$$(1+\eta)\frac{d^2E_0}{d\xi^2}=\frac{E_0D_1^2}{1+\eta}+\Lambda E_0(1-I_0) , \tag{49}$$

as can be derived from Eqs. (19), (21), and (22), Eqs. (46) and (47) can be written in terms of I_1 and D_2 as

$$\frac{dI_1}{d\xi}=\frac{1}{1+\eta}\left[2D_1I_1+2I_0D_2-\frac{2\eta I_0}{1+\eta}\left[\frac{D_1^2}{1+\eta}+\Lambda E_0(1-I_0)\right]\right] , \tag{50}$$

$$\frac{dD_2}{d\xi}=-\Lambda I_1-D_1-\tilde{\Lambda}\eta I_0D_1 . \tag{51}$$

In numerical calculations, it is more convenient to introduce

$$\tilde{\xi}\equiv 2\sqrt{\tilde{\Lambda}}\xi=\int_{I_{\min}}^{I_0(\xi)}\frac{dy}{y\sqrt{\ln y-\ln I_{\max}+I_{\max}-y}} , \tag{52}$$

$$\tilde{D}_1\equiv\frac{D_1}{\sqrt{\Lambda(1+\eta)}}=\pm\sqrt{\ln I_0-\ln I_{\min}+I_{\min}-I_0} , \tag{53}$$

$$\tilde{D}_2\equiv\frac{D_2}{\sqrt{\Lambda(1+\eta)}} . \tag{54}$$

In terms of these variables, Eqs. (50) and (51) are

$$\frac{dI_1}{d\tilde{\xi}}=\tilde{D}_1 I_1+I_0\tilde{D}_2-\frac{\eta\sqrt{\tilde{\Lambda}}}{1+\eta}I_0(\tilde{D}_1^2+1-I_0)\ , \tag{55}$$

$$\frac{d\tilde{D}_2}{d\tilde{\xi}}=-\frac{I_1}{2}-\frac{\tilde{D}_1}{2\sqrt{\tilde{\Lambda}}}(1+\eta\tilde{\Lambda}I_0)\ . \tag{56}$$

These equations can be written in vectorial form. To this end, we define

$$\hat{A}\equiv\begin{bmatrix}\tilde{D}_1 & I_0\\ -1/2 & 0\end{bmatrix}, \tag{57}$$

$$\mathbf{F}\equiv\begin{bmatrix}I_1\\ \tilde{D}_2\end{bmatrix}, \tag{58}$$

$$\mathbf{f}\equiv-\begin{bmatrix}\frac{2\eta}{1+\eta}\tilde{\Lambda}I_0(\tilde{D}_1^2+1-I_0)\\ \tilde{D}_1(1+\eta\tilde{\Lambda}I_0)\end{bmatrix}. \tag{59}$$

Then Eqs. (55) and (56) take the form

$$\frac{d\mathbf{F}}{d\tilde{\xi}}=\hat{A}\mathbf{F}+\mathbf{f}\ . \tag{60}$$

It is easy to see that for given $I_{\min}$ (or $I_{\max}$), both $I_0(\tilde{\xi})$ and $D_1(\tilde{\xi})$ are $\tilde{T}$-periodic functions, where, due to Eqs. (40) and (52), $\tilde{T}$ is given by

$$\tilde{T}=2\int_{I_{\min}}^{I_{\max}}\frac{dy}{\sqrt{\ln y-\ln I_{\min}+I_{\min}-y}}\ . \tag{61}$$

By the definitions, Eqs. (57) and (59), $\hat{A}$ and $\mathbf{f}$ are also $\tilde{T}$-periodic functions. Generally, this does not ensure that Eq. (60) has a $\tilde{T}$-periodic function, as required by the periodic ring boundary conditions.

To find the condition that the inhomogeneous Eq. (60) has a $\tilde{T}$-periodic solution, we refer ourselves to the mathematical theorems introduced in Appendix A.[41] Given any $0<I_{\min}<1$, it can be verified by using a Runge-Kutta procedure that the corresponding homogeneous system of Eq. (60), i.e.,

$$\frac{d\mathbf{y}}{d\tilde{\xi}}=\hat{A}\mathbf{y} \tag{62}$$

always has a $\tilde{T}$-periodic solution. Therefore, according to Theorem II, the adjoint system

$$\frac{d\mathbf{z}}{d\tilde{\xi}}=-\hat{A}^*\mathbf{z} \tag{63}$$

also has a $\tilde{T}$-periodic solution $\mathbf{z}(\tilde{\xi})$, and Eq. (60) has a $\tilde{T}$-periodic solution if and only if

$$\langle\mathbf{z}|\mathbf{f}\rangle=0\ , \tag{64}$$

where the operation $\langle\ |\ \rangle$ is defined in Appendix A.

E. η as a function of Λ

Using a Runge-Kutta procedure, we can show that for any given η, $\langle\mathbf{z}|\mathbf{f}\rangle$ as a function of pumping Λ has only one zero point, see Fig. 2. Therefore, the periodicity condition (64) defines a function $\Lambda=\Lambda(\eta)$.

Numerical solutions of Eq. (64) show that this function is given by

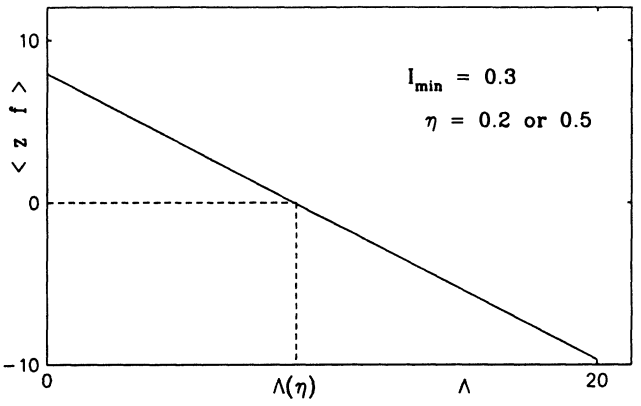

FIG. 2. For given η, $\langle\mathbf{z}|\mathbf{f}\rangle$ as a function of Λ has just one zero point, which uniquely defines the function $\Lambda=\Lambda(\eta)$.

$$\Lambda=\frac{(1+\eta)^2}{\eta(1-\eta)}\ . \tag{65}$$

In fact, this simple relation is first encountered in the linear stability analysis of the self-pulsing solution, which will be discussed in Sec. IV, and then is numerically verified to be precisely the function $\Lambda(\eta)$ defined by Eq. (64).

Equation (65) yields the following two solutions:

$$\eta_\pm=\frac{1}{2(1+\Lambda)}[\Lambda-2\pm\sqrt{\Lambda(\Lambda-8)}]\ . \tag{66}$$

Since for a steady pulse the phase velocity (and hence η) must be a real number, Λ has to exceed the minimum second threshold given by Eq. (76), which is equal to 8 in the limit $\gamma\to 0$. Thus, it follows from Eq. (66) that

$$0<\eta_-\le 1/3\le\eta_+<1 \tag{67}$$

and

$$\lim_{\Lambda\to\infty}\eta_-=0,\quad \lim_{\Lambda\to\infty}\eta_+=1\ . \tag{68}$$

η as a function of Λ is illustrated in Fig. 3(a). In what follows, we denote a function $f(\eta)$ as $f_\pm$ according to $\eta=\eta_\pm$.

According to Eq. (66)–(68), it follows from Eq. (10) that

$$v_\pm(\Lambda)=\frac{2c(1+\Lambda)}{2(1+\Lambda)-\chi[\Lambda-2\pm\sqrt{\Lambda(\Lambda-8)}]}\ , \tag{69}$$

$$c<v_-\le\frac{c}{1-\chi/3}\le v_+\ , \tag{70}$$

$$\lim_{\Lambda\to\infty}v_-(\Lambda)=c,\quad \lim_{\Lambda\to\infty}u_+(\Lambda)=\frac{c}{1-\chi}\ . \tag{71}$$

v/c as a function of Λ is illustrated in Fig. 3(b), where we see that v_- decreases with Λ, while v_+ increases with Λ. The physical meaning of the inequality $v_\pm > c$ was suggested by Risken and Nummedal, i.e., the photons are produced at the front edge of the pulse and travel with velocity $(v-c)$ through the pulse to be finally absorbed at the trailing edge of the pulse; thus the velocity of the pulse propagating in the medium never exceeds the velocity of light.

In terms of Eq. (32), $\tilde{\Lambda}$ is also a function of Λ,

$$\tilde{\Lambda}_\pm = \frac{3\Lambda \mp \sqrt{\Lambda(\Lambda-8)}}{4} . \tag{72}$$

With Eqs. (69) and (72), the self-pulsing solution Eq. (41) can be written as

$$\frac{c}{v_\pm}\sqrt{2\tilde{\Lambda}_\pm} = \left[\frac{3\Lambda \pm \sqrt{\Lambda(\Lambda-8)}}{2}\right]^{1/2} \times \left[1 - \frac{2\chi}{\Lambda - 2 \pm \sqrt{\Lambda(\Lambda-8)}}\right] = \frac{\sqrt{2}N}{T_s}\int_{I_{\min}}^{I_{\max}} \frac{dy}{\sqrt{\ln y - \ln I_{\min} + I_{\min} - y}} . \tag{73}$$

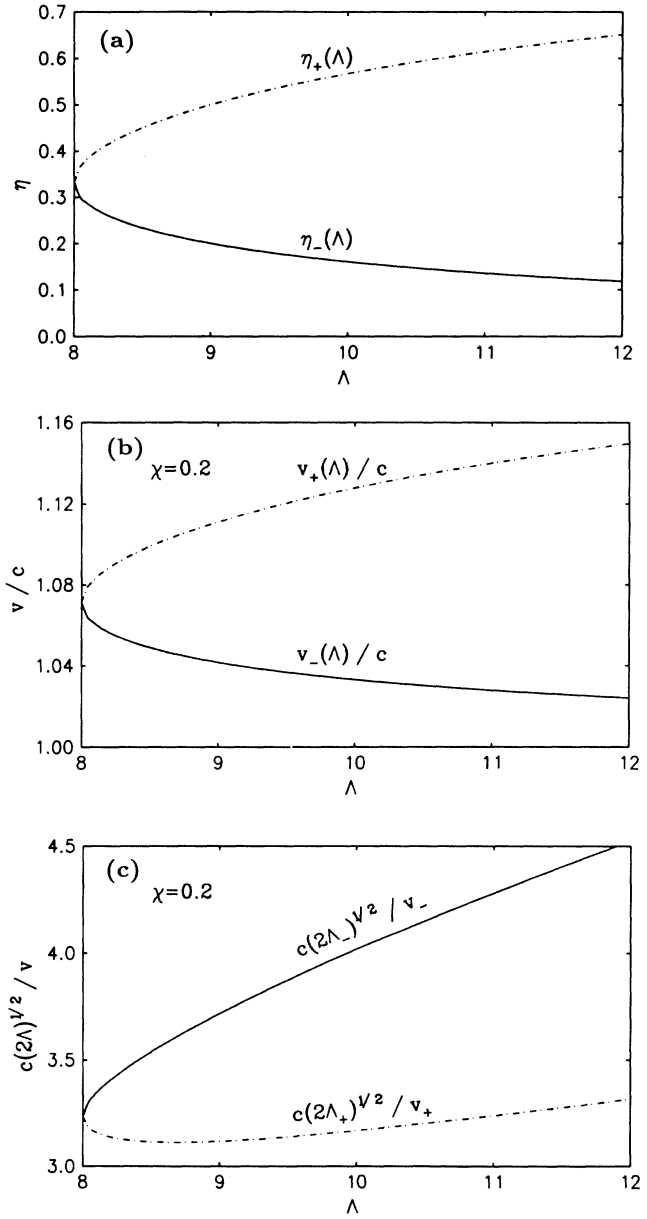

FIG. 3. (a)–(c), $\eta_\pm$, $v_\pm/c$, and $c\sqrt{2\tilde{\Lambda}}/v_\pm$ as functions of Λ.

$c\sqrt{2\tilde{\Lambda}}/v$ as a function of Λ is illustrated in Fig. 3(c). The amplitude $I_{\max}$ as a function of Λ has a behavior similar to $c\sqrt{2\tilde{\Lambda}_\pm}/v_\pm$, i.e., $I_{\max}(\Lambda)$ increases (or decreases) in the region where $c\sqrt{2\tilde{\Lambda}_\pm}/v_\pm$ increases (or decreases). Typical examples will be shown in Fig. 5 in Sec. III. From Figs. 3(b) and 3(c), we find that the η_+ self-pulsing solutions have the following unphysical properties.

First, if the η_+ self-pulsing solution exists in the decreasing region of $c\sqrt{2\tilde{\Lambda}_+}/v_\pm$, see Fig. 3(c), then the oscillating amplitude $I_{\max}$ decreases with Λ.

Second, if it exists in the increasing region, then, on the one hand, the pulsewidth becomes narrower as the pump Λ is increased; on the other hand, we see from Fig. 3(b) that the phase velocity v_+ becomes larger. This behavior contradicts the physical picture proposed by Risken and Nummedal, which implies that a narrower pulse corresponds to a smaller phase velocity.

As is apparent in Fig. 3, the η_- self-pulsing solution does not share these unphysical properties. Therefore, the physical self-pulsing solutions correspond to $\eta=\eta_-$. This conclusion is supported by the stability argument to be discussed in the following sections.

At this stage, we have seen that in order to determine a self-pulsing solution for given Λ we still need to determine the pulse number N. We shall show in Sec. III that N turns out to be the RNGH unstable mode index. Therefore the self-pulsing solution is uniquely determined for a given laser system.

We mention in passing (the proof will not be given here) that the self-pulsing solution derived in this section can also be obtained by using Fourier expansions on the basis of a single frequency component and its harmonics. Therefore, these self-pulsing solutions consist of just one basic frequency apart from its harmonics. This basic component corresponds to a newly excited cavity mode above the second threshold, which leads to the RNGH instability of the stationary solution; see also Ref. 24.

III. RELATIONS BETWEEN THE SELF-PULSING SOLUTIONS AND THE RNGH INSTABILITY

We have seen in Eq. (73) that an N-pulse solution is determined by the quantity $\sqrt{2\tilde{\Lambda}_\pm}c/v_\pm$ corresponding to $\eta=\eta_\pm$. In this section, we shall show that these two quantities turn out to be the lower and upper boundaries of the RNGH-instability region for the stationary solution. Based on this connection, we shall show that for a stable self-pulsing solution the pulse number N is largely

limited by the requirement of stability, and that the self-pulsing phenomena depend on how the RNGH instability appears. If the RNGH unstable mode lies on the upper boundary, the corresponding self-pulsing solution is supercritical; if it lies on the lower boundary, the corresponding self-pulsing solution is subcritical and the system is bistable.

The RNGH instability can be described as follows. Let us consider the linear stability of the stationary solution, i.e., the unit solution of the Maxwell-Bloch equations (6)–(8), against small perturbations. Under periodic boundary condition, the perturbations can be expanded into cavity modes $\exp(i\alpha_m \xi/c)$, where the wave vector

$$\alpha_m = \frac{2m\pi}{T_s}, \quad m = 0, \pm 1, \ldots . \tag{74}$$

Without loss of generality, we suppose $m \geq 0$ in the following discussions. As shown in Refs. 1 and 2, the RNGH instability occurs if a cavity mode α_m falls in the unstable region $(\alpha_{\min}, \alpha_{\max})$ for given Λ. In the limit $\gamma \to 0$, the upper and lower boundaries $\alpha_{\max}$ and $\alpha_{\min}$ of this unstable region are given by

$$\alpha_{\max,\min} = \left[\frac{3\Lambda \pm \sqrt{\Lambda(\Lambda-8)}}{2} \right]^{1/2} \times \left[1 - \frac{2\chi}{\Lambda - 2 \pm \sqrt{\Lambda(\Lambda-8)}} \right] . \tag{75}$$

Obviously, the unstable region exists only for Λ greater than the minimum second threshold

$$\Lambda_{\mathrm{RNGH,min}} \equiv 4 + 3\gamma + 2\sqrt{2(1+\gamma)(2+\gamma)} = 8, \quad \gamma \to 0 . \tag{76}$$

The unstable mode touches the unstable boundary usually at a pump higher than $\Lambda_{\mathrm{RNGH,min}}$. The exact second threshold Λ_{RNGH} and the wave vector of the unstable mode α_{RNGH} can be determined in the following way.[13] For given T_s, let us draw straight lines $\alpha = \alpha_m$ for different integers m, which intersect at the curves $\alpha_{\min,\max}(\Lambda)$ and yield a set of points (Λ_m, α_m)

$$\alpha_m = \alpha_{\max}(\Lambda_m), \quad \text{or } \alpha_m = \alpha_{\min}(\Lambda_m) , \tag{77}$$

see Fig. 4. Then, the second threshold is given by

$$\Lambda_{\mathrm{RNGH}} = \min(\Lambda_m) \tag{78}$$

and the corresponding mode is α_{RNGH}. Define N_{RNGH} as the mode number, i.e.,

$$\alpha_{\mathrm{RNGH}} = \frac{2\pi N_{\mathrm{RNGH}}}{T_s} . \tag{79}$$

For convenience, we shall call $(\alpha_{\mathrm{RNGH}}, \Lambda_{\mathrm{RNGH}})$ the RNGH intersection, and all the other ones the non-RNGH intersections.

As shown in Figs. 4(a) and 4(b), the RNGH intersection may lie either on the upper boundary or on the lower boundary of the unstable region, depending on the system parameters T_s and χ. For $\Lambda > \Lambda_{\mathrm{RNGH}}$, the α_{RNGH} mode enters the unstable region and the stationary solution becomes unstable.

Now let us study the relation between the RNGH instability and the self-pulsing solutions. Comparing Eq. (75) to Eq. (73), we find that

$$\alpha_{\min} = \frac{c}{v_+}\sqrt{2\tilde{\Lambda}_+}, \quad \alpha_{\max} = \frac{c}{v_-}\sqrt{2\tilde{\Lambda}_-} . \tag{80}$$

Therefore, the self-pulsing solution Eq. (73) can be written in the form

$$\frac{\sqrt{2}N}{T_s} \int_{I_{\min}}^{I_{\max}} \frac{dy}{\sqrt{\ln y - \ln I_{\min} + I_{\min} - y}} = \begin{cases} \alpha_{\max}(\Lambda) & \text{if } \eta = \eta_- \\ \alpha_{\min}(\Lambda) & \text{if } \eta = \eta_+ \end{cases} . \tag{81}$$

Now we show that each self-pulsing solution in the limit $I_{\min} \to 1$ corresponds to an intersection shown in Fig. 4. In fact, using a Taylor expansion, it is easy to calculate

$$\lim_{I_{\min} \to 1-0} \int_{I_{\min}}^{I_{\max}} \frac{dy}{\sqrt{\ln y - \ln I_{\min} + I_{\min} - y}} = \sqrt{2}\pi . \tag{82}$$

Therefore, in this limit, Eq. (81) becomes equivalent to Eq. (77), which means that a self-pulsing solution approaches the stationary solution at the corresponding in-

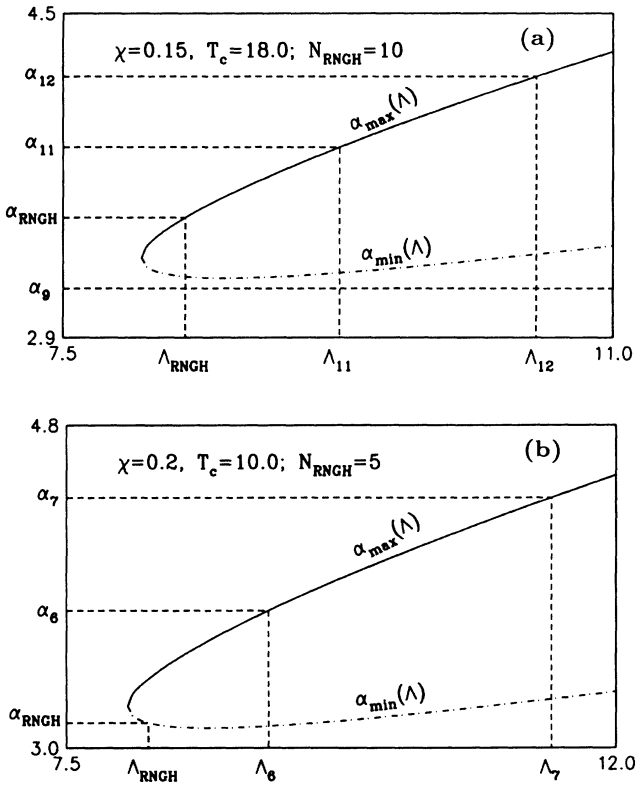

FIG. 4. RNGH unstable region for the stationary laser (Refs. 1 and 2) and the graphical solution for Λ_{RNGH} and α_{RNGH}. As shown in (a) and (b), the RNGH intersection $(\Lambda_{\mathrm{RNGH}}, \alpha_{\mathrm{RNGH}})$ may either lie on the upper or the lower boundary of the unstable region.

tersection, or, in other words, the self-pulsing arises when a cavity mode touches the unstable region of the stationary solution. This relation suggests the following conclusions concerning the stability of the self-pulsing solutions in the vicinity of the intersections.

(a) All the self-pulsing solutions corresponding to the non-RNGH intersections, including η_- and η_+ solutions, are unstable.

For the self-pulsing solution corresponds to the RNGH intersection, we have the following.

(b) If the RNGH intersection lies on the upper boundary of the unstable region, the corresponding solution, i.e., the η_- solution with $N=N_{\mathrm{RNGH}}$, is a stable supercritical periodic solution, see Fig. 5(a).

(c) If the RNGH intersection lies on the lower boundary of the unstable region, the corresponding solution, i.e., the η_+ solution with $N=N_{\mathrm{NRGH}}$, is a unstable subcritical solution; however, the η_- solution with $N=N_{\mathrm{RNGH}}$ is a stable subcritical periodic solution, provided that the amplitude $L_{\max}$ at $\Lambda=\Lambda_{\mathrm{RNGH}}$ satisfies $I_{\max}<I_{\max,N_{\mathrm{RNGH}}}$, where $L_{\max,N}$ is defined in Sec. VI A; and in this case, both the self-pulsing and the stationary solution can be stable, see Fig. 5(b); if $I_{\max}>I_{\max,N_{\mathrm{RNGH}}}$ at $\Lambda=\Lambda_{\mathrm{RNGH}}$, there is no stable self-pulsing at all.

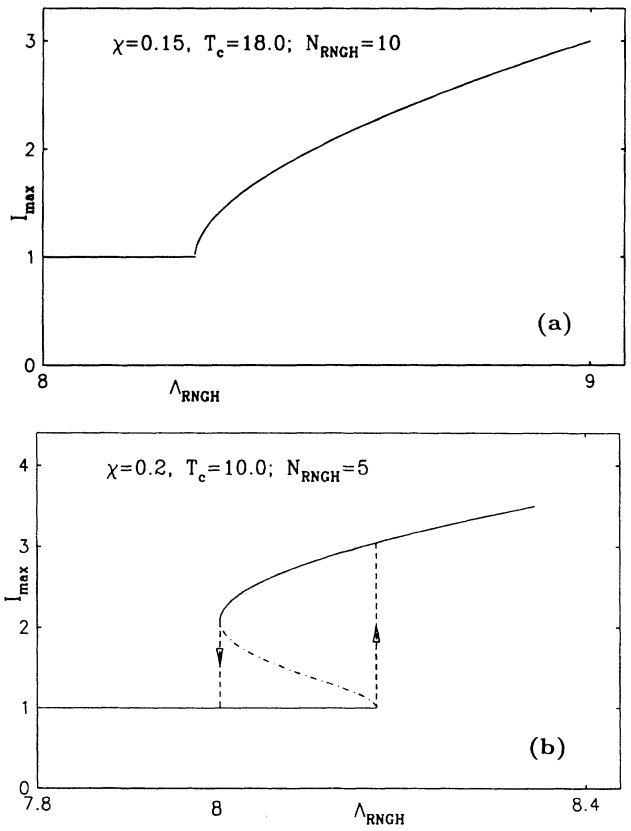

FIG. 5. Appearance of self-pulsing depends on how the RNGH instability occurs. (a) If $(\Lambda_{\mathrm{RNGH}},\alpha_{\mathrm{RNGH}})$ lies on the upper boundary, the self-pulsing solution is supcritical; (b) if it lies on the lower boundary, the self-pulsing solution is subcritical. The dot-dashed curve is the unphysical η_+ solution. In this case the system has bistability.

Let us first discuss conclusion (a). By the definition of Λ_{RNGH}, the inequality $\Lambda>\Lambda_{\mathrm{RNGH}}$ holds in the vicinity of the non-RNGH intersections. Therefore, the self-pulsing solutions approach the already unstable stationary solution at the intersections and must diverge with it. Such kinds of instabilities are expected, because the corresponding self-pulsing solutions do not contain the newly excited (unstable) mode. In this sense, these instabilities have the same origin as the RNGH instability of the stationary solution. Therefore, we call them RNGH-type instabilities. It should be noted that the RNGH-type instabilities refer to the self-pulsing solutions, while the RNGH instability refers to the stationary solution.

Now we discuss conclusions (b) and (c). In the case of (b), the self-pulsing solution arises just at the point where the stationary solution loses its stability. Therefore, at least in the vicinity of the RNGH intersection, this is a stable supercritical solution, see Figs. 4(a) and 5(a).

In the case of (c), there is a pair of solutions with $N=N_{\mathrm{RNGH}}$. One is the η_+ self-pulsing solution, of which the oscillating amplitude decreases when Λ increases from Λ_{2nd} to Λ_{RNGH} and approaches the stationary solution at Λ_{RNGH}. Since the stationary solution is stable for $\Lambda<\Lambda_{\mathrm{RNGH}}$, the η_+ self-pulsing solution must be trapped by it and hence is unstable. The other is the η_- solution, which has the same amplitude as the η_+ solution at $\Lambda=\Lambda_{\mathrm{2nd}}$, but then its amplitude increases with Λ. According to the general bifurcation theory, we expect that this periodic solution is stable. However, there exists another kind of instability which occurs for $I_{\max}>I_{\max,N_{\mathrm{RNGH}}}$, as we shall discuss in Sec. VI A.

The linear stability analysis presented in Secs. IV–VI shows the following. (1) Conclusion (a) holds not only in the vicinity of the interactions, where the amplitude of the self-pulsing is small, but also for arbitrary pump; (2) conclusion (b) holds for $\Lambda_{\mathrm{RNGH}}<\Lambda<\Lambda_{N,C}$, where $\Lambda_{N,C}$ is the so-called large-amplitude instability threshold to be introduced in Secs. IV–VI; and (3) for conclusion (a), we cannot show by the linear stability analysis that the η_+ solution is unstable, because the Floquet exponent vanishes for the spatially homogeneous perturbation. A definite answer to this question can only be given when one goes to the nonlinear regime, which will not be discussed here. But, because of the unphysical properties of the $\eta_\pm$ solutions, we believe that this solution is unstable.

Now we still need to discuss self-pulsing solutions which do not correspond to any intersections of the RNGH unstable region. These solutions generally have a smaller pulse number N and larger oscillating amplitude, as can be seen from Eq. (73). Therefore, most of them are excluded by the large-amplitude instability. By using the numerical procedure for linear stability analysis presented in Secs. IV–VI, we could show that, in case (b), there may (or may not) exist a stable η_- solution with $N=N_{\mathrm{RNGH}}-1$ for $\Lambda_{\mathrm{2nd}}<\Lambda<\Lambda_{N,C}$ $(<\Lambda_{\mathrm{RNGH}})$; and in case (c), the only stable solution is that described in conclusion (c).

It is worth pointing out that, though the relation Eq. (81) is obtained in the limit $\gamma\to 0$, it suggests that the

self-pulsing solutions of Eqs. (11)–(13), where γ may be any finite number, have the form

$$\alpha_{\min,\max}(\Lambda,\gamma,\chi)=\frac{2\pi N}{T_s}f(I_{\min},\gamma,\chi) , \tag{83}$$

where the function $f(I_{\min},\gamma,\chi)$ satisfies

$$\lim_{I_{\min}\to 1} f(I_{\min},\gamma,\chi)=1 . \tag{84}$$

If this is true, the task to find the general solution of Eqs. (11)–(13) will become easier.

IV. LINEAR STABILITY ANALYSIS OF THE SELF-PULSING SOLUTION

This section is divided into four parts. In the first part, Sec. IV A, the general approach based on the full set of the Maxwell-Bloch equations is formulated in order to analyze the linear stability of the space-time–dependent self-pulsing solutions. The Floquet exponents which characterize the linear stability of the self-pulsing solution are found to satisfy two independent sets of equations.

Then the five Floquet exponents for a given cavity mode are discussed in the limits $\chi\to 0$ and $\gamma\to 0$. In the second part, it is shown that three of the five Floquet exponents always have negative real parts, which in fact describes the stability of the linear response of a passive medium to an external field.

One of the remaining two Floquet exponents is analytically solved in Sec. IV C and the real part is found to be nonpositive. Therefore, for a given cavity mode, only one Floquet exponent may have a positive real part. Procedures to calculate this Floquet exponent are presented in Sec. IV C, which can only be handled numerically in the general case.

A. The general formalism

Since the self-pulsing solutions up to the order of γ depend explicitly on the intensities I_0 and I_1, but not on the phases of the fields E and P, we assume, without loss of generality, the self-pulsing solution to be real quantities

$$E=E^*, \quad P=P^* . \tag{85}$$

In order to analyze the linear stability of the self-pulsing solutions, we study the perturbations δF, where F may stand for E, E^*, P, P^*, and D. In the linear regime, we obtain from the Maxwell-Bloch equations (6)–(8)

$$\sqrt{\gamma}\left[\frac{\partial\delta E}{\partial\tau}+c\frac{\partial\delta E}{\partial\xi}\right]=\chi(\delta P-\delta E) , \tag{86}$$

$$\sqrt{\gamma}\frac{\partial\delta P}{\partial\tau}=D\delta E+E\delta D-\delta P , \tag{87}$$

$$\frac{\partial\delta D}{\partial\tau}=-\sqrt{\gamma}\left[\delta D+\frac{\Lambda}{2}[E(\delta P+\delta P^*)+P(\delta E+\delta E^*)]\right] . \tag{88}$$

This is a linear differential system with periodic coefficients and is to be solved under the spatially periodic boundary condition. According to the Floquet theorem,[8,41] the solution of Eqs. (86)–(88) generally has the form

$$\delta F(\xi,\tau)=e^{\lambda\tau}f(\xi,\tau) , \tag{89}$$

where Λ is the Floquet exponent characterizing the linear stability and $f(\xi,\tau)$ satisfies the spatial- and temporal-periodicity condition

$$f(\xi+mT_s,\tau+nT)=f(\xi,\tau) , \tag{90}$$

where m and n are integers, T_s describes the spatial period of the ring cavity, and T the period of the self-pulsing solution, see Eq. (39). f defined in Eq. (89) may be any one of e, e_c, p, p_c, or d, corresponding to E, E^*, P, P^*, or D. Inserting Eq. (89) into Eqs. (86)–(88), we obtain

$$\sqrt{\gamma}\left[\lambda+\frac{\partial}{\partial\tau}+c\frac{\partial}{\partial\xi}\right]e=\chi(p-e) , \tag{91}$$

$$\sqrt{\gamma}\left[\lambda+\frac{\partial}{\partial\tau}\right]p=De+Ed-p , \tag{92}$$

$$\left[\lambda+\frac{\partial}{\partial\tau}\right]d=-\sqrt{\gamma}\left[d+\frac{\Lambda}{2}[E(p+p_c)+P(e+e_c)]\right] . \tag{93}$$

In order to solve the partial differential equations, it is usual to expand the perturbations into cavity modes. However, since the self-pulsing solution is a space-dependent function, infinitely many cavity modes would be involved in the resulting ordinary differential equations. This difficulty can be overcome by transforming the coordinate system ξ,τ into (ξ,ξ) because in the new system the self-pulsing solution depends only on $\xi\equiv\tau-\xi/v$, as defined in Eq. (9), but not on ξ. Therefore, the perturbations with a specific cavity mode form a closed set of equations and the Floquet exponent can be analyzed in the subspace.

By the definitions, Eq. (4), the derivatives in the two coordinate systems have the following relations:

$$\frac{\partial}{\partial\tau}=\frac{\partial}{\partial\xi'}\frac{\partial}{\partial\xi}=\frac{\partial}{\partial\xi}-\frac{1}{v}\frac{\partial}{\partial\xi} . \tag{94}$$

Therefore, in the (ξ,ξ) system, Eqs. (91)–(93) take the form

$$\sqrt{\gamma}\left[\lambda+\eta\chi\frac{\partial}{\partial\xi}+c\frac{\partial}{\partial\xi}\right]e=\chi(p-e) , \tag{95}$$

$$\sqrt{\gamma}\left[\lambda+\frac{\partial}{\partial\xi}\right]p=De+Ed-p , \tag{96}$$

$$\left[\lambda+\frac{\partial}{\partial\xi}\right]d=-\sqrt{\gamma}\left[d+\frac{\Lambda}{2}[E(p+p_c)+P(e+e_j)]\right] . \tag{97}$$

In accord with Eq. (90), the solutions of these equations have to satisfy the following periodicity condition:

$$f(\zeta+mT_s,\xi+nT)=f(\zeta,\xi) . \tag{98}$$

Since the coefficients in Eqs. (95)–(97) do not depend on ζ, we can assume that (e,e_c,p,p_c,d) in the (ζ,ξ) system have the form

$$f(\zeta,\xi)=e^{i\alpha_m\zeta/c}f(\xi), \quad \alpha_m\equiv\frac{2\pi m}{T_s} , \tag{99}$$

where $f(\xi)$ satisfies

$$f(\xi+nT)=f(\xi) . \tag{100}$$

Inserting Eq. (99) into Eqs. (95)–(97), we obtain for each cavity mode the following ordinary differential equations:

$$\sqrt{\gamma}\left[\lambda-i\alpha_m+\eta\chi\frac{d}{d\xi}\right]e=\chi(p-e) , \tag{101}$$

$$\sqrt{\gamma}\left[\lambda+\frac{d}{d\xi}\right]p=De+Ed-p , \tag{102}$$

$$\left[\lambda+\frac{d}{d\xi}\right]d=-\sqrt{\gamma}\left[d+\frac{\Lambda}{2}[E(p+p_c)+P(e+e_c)]\right] . \tag{103}$$

Now we show that these equations can be separated into two independent sets of equations. In fact, introducing

$$e_\pm\equiv e\pm e_c, \quad p_\pm\equiv p\pm p_c , \tag{104}$$

we find from Eqs. (101)–(103) that

$$\sqrt{\gamma}\left[\lambda+i\alpha_m+\eta\chi\frac{d}{d\xi}\right]e_-=\chi(p_--e_-) , \tag{105}$$

$$\sqrt{\gamma}\left[\lambda+\frac{d}{d\xi}\right]p_-=De_--p_- , \tag{106}$$

$$\sqrt{\gamma}\left[\lambda+i\alpha_m+\eta\chi\frac{d}{d\xi}\right]e_+=\chi(p_+-e_+) , \tag{107}$$

$$\sqrt{\gamma}\left[\lambda+\frac{d}{d\xi}\right]p_+=De_+-p_++2Ed , \tag{108}$$

$$\left[\lambda+\frac{d}{d\xi}\right]d=-\sqrt{\gamma}\left[d+\frac{\Lambda}{2}(Ep_++Pe_+)\right] . \tag{109}$$

These two sets of equations subject to the periodicity condition (100) determine the Floquet exponents λ. The self-pulsing solution is stable if $\mathrm{Re}\lambda<0$ for all α_m and it is unstable if $\mathrm{Re}\lambda>0$ for some α_m.

The Floquet exponents λ are studied in the following sections in the limits $\chi\to0$ and $\gamma\to0$. In this case, λ can be expanded into the χ series

$$\lambda=\lambda_0+\lambda_1\chi+\cdots . \tag{110}$$

B. Floquet exponents which always have negative real parts

Now, we show that, similar to the linear stability analysis for the stationary solution, three Floquet exponents always have negative real parts. One of them comes from Eqs. (105) and (106), the other two from Eqs. (107)–(109).

To this end, we assume $\chi\to0$ and $e_-=0$. Under this assumption, Eq. (105) becomes an identity and Eq. (105) takes the form

$$\frac{dp_-}{d\xi}=-\left[\lambda_0+\frac{1}{\sqrt{\gamma}}\right]p_- . \tag{111}$$

Since $p_-(\xi)$ is a periodic function, the Floquet exponent has to satisfy

$$\mathrm{Re}\lambda_0=-\frac{1}{\sqrt{\gamma}}<0 . \tag{112}$$

Now, let us consider Eqs. (107)–(109). Making use of the assumption $\chi\to0$ and $e_+=0$, we find that Eq. (107) becomes an identity and Eqs. (108) and (109) take the form

$$\sqrt{\gamma}\left[\lambda+\frac{d}{d\xi}\right]p_+=2Ed-p_+ , \tag{113}$$

$$\left[\lambda+\frac{d}{d\xi}\right]d=-\sqrt{\gamma}\left[d+\frac{\Lambda E}{2}p_+\right] . \tag{114}$$

In order to show that these two Floquet exponents have negative real parts in the limit $\gamma\to0$, we expand λ_0 with respect to γ

$$\lambda_0=\frac{\lambda_{0,-1}}{\sqrt{\gamma}}+\lambda_{0,0}+\lambda_{0,1}\sqrt{\gamma}+\cdots . \tag{115}$$

Inserting this expansion into Eqs. (113) and assuming $\lambda_{0,-1}\neq0$, we find, in the lowest order of γ, that

$$\lambda_{0,-1}p_+=2Ed-p_+\lambda_{0,-1}d=0 , \tag{116}$$

which yields $d=0$ and $\lambda_{0,-1}=-1$, i.e.,

$$\lambda_0=-\frac{1}{\sqrt{\gamma}}+\cdots . \tag{117}$$

In the case $\lambda_{0,-1}=0$, we can show that $\mathrm{Re}\lambda_{0,0}=0$ and $\lambda_{0,1}<0$. To this end, we expand p_+ and d into the γ series

$$p_+=p_{+,0}+p_{+,1}\sqrt{\gamma}+\cdots , \tag{118}$$

$$d=d_0+d_1\sqrt{\gamma}+\cdots . \tag{119}$$

In the zeroth order, Eqs. (113) and (114) are

$$p_{+,0}=2E_0d_0 , \tag{120}$$

$$\left[\lambda_{0,0}+\frac{d}{d\xi}\right]d_0=0 . \tag{121}$$

Since $d_0(\xi)$ is a T-periodic function, $\lambda_{0,0}$ must be equal to $\lambda_{0,0}=i2\pi n/T$, where n is an integer. Thus the solutions in the zeroth order are

$$d_0(\xi)=e^{-i2\pi n\xi/T},\quad p_{+,0}(\xi)=2E_0(\xi)e^{-i2\pi n\xi/T}. \tag{122}$$

Since $\mathrm{Re}\lambda_{0,0}=0$, we need to calculate $\lambda_{0,1}$. To this end, it is sufficient to solve Eq. (114) in the first order. Inserting Eq. (119) into Eq. (114) and making use of $\lambda_{0,0}$ and Eq. (122), we obtain

$$\left[\frac{i2\pi n}{T}+\frac{d}{d\xi}\right]d_1(\xi) =-[\lambda_{1,1}+1+\Lambda I_0(\xi)]e^{-i2\pi n\xi/T}. \tag{123}$$

Thus, for $d_1(\xi)$ to be a T-periodic function, it is necessary that

$$\int_0^T[\lambda_{1,1}+1+\Lambda I_0(\xi)]d\xi=0. \tag{124}$$

Since the average value of $I_0(\xi)$ is unitary, it follows from Eq. (124) that $\lambda_{0,1}+1+\Lambda=0$, i.e.,

$$\lambda_0=-(1+\Lambda)\sqrt{\gamma}+\cdots. \tag{125}$$

We have thus proved, in the lowest order of χ and γ, that three Floquet exponents always have negative real parts, see Eqs. (112), (117), and (125). The corresponding perturbations are of the form $(e,e_c,p,p_c,d)=(0,0,p,p_c,d)$. Physically, since the Maxwell equation is not involved in the above analysis, what we have proven is just the linear stability of the response of a passive system upon an external periodic electric field. Therefore, the conclusion that three Floquet exponents always have negative real parts may be true for finite χ and γ, as in the case of stationary solutions.[34,42,43]

In the following sections, we shall discuss the other two Floquet exponents corresponding to perturbations $(e,e_c)\neq(0,0)$. In the limit $\chi\to0$, we find from Eqs. (105) and (107) that $\lambda_0=-i\alpha_m$, where λ_0 is defined in Eq. (110). Thus, the Floquet exponents take the form

$$\lambda=i\alpha_m+\lambda_1\chi+\cdots. \tag{126}$$

Therefore, in order to study the linear stability in the limit $\chi\to0$, we need to calculate λ_1. This will be done in Secs. IV A and IV B.

C. The Floquet exponent related to (e_-,p_-)

Inserting Eq. (126) into Eqs. (105) and (106), and keeping the lowest-order terms in χ, we find

$$\sqrt{\gamma}\left[\lambda_1+\eta\frac{d}{d\xi}\right]e=(p-e), \tag{127}$$

$$\sqrt{\gamma}\left[-\alpha_m+\frac{d}{d\xi}\right]p=De-p, \tag{128}$$

where (e,p) stands for (e_-,p_-). In the limit $\gamma\to0$, λ_1 and e,p can be expanded into the $\sqrt{\gamma}$ series, see also Eqs. (115), (118), and (119),

$$f=f_0+f_1\sqrt{\gamma}+\cdots. \tag{129}$$

In the zeroth order, we find from Eqs. (127) and (128) that

$$e_0=p_0. \tag{130}$$

In the first order, Eqs. (127) and (128) are

$$\left[\lambda_{1,0}+\eta\frac{d}{d\xi}\right]e_0=p_1-e_1, \tag{131}$$

$$\left[-i\alpha_m+\frac{d}{d\xi}\right]p_0=D_1e_0-(p_1-e_1). \tag{132}$$

Eliminating (p_1-e_1) by adding Eq. (131) to Eq. (132) and taking Eq. (130) into account, we obtain

$$(1+\eta)\frac{de_0}{d\xi}=(i\alpha_m-\lambda_{1,0}+D_1)e_0. \tag{133}$$

The solution is

$$e_0(\xi)=e_0(0)\exp\left[\frac{i\alpha-\lambda_{1,0}}{1+\eta}\xi+\frac{1}{1+\eta}\int_0^\xi D_1(\xi)d\xi\right]. \tag{134}$$

From Eqs. (21) and (25), it is easy to show that

$$\int_0^\xi D_1(\xi)d\xi=\frac{1+\eta}{2}\ln\frac{I_0(\xi)}{I_{\min}} \tag{135}$$

is a T-periodic function. Therefore, from Eq. (134), that $e_0(\xi)$ is a T-periodic function requires that

$$\frac{i\alpha_m-\lambda_{1,0}}{1+\eta}=\frac{i2\pi n}{T}. \tag{136}$$

By the definitions of T and α_n, $2\pi n/T=2\pi nN/T_s=\alpha_{nN}$, we obtain

$$\lambda_{1,0}=i[\alpha_m-(1+\eta)\alpha_{nN}]. \tag{137}$$

Since $\mathrm{Re}\lambda_{1,0}=0$, we need to calculate $\lambda_{1,1}$ to determine the linear stability. To this end, let us consider Eqs. (127) and (128) in the order of γ,

$$\left[\lambda_{1,0}+\frac{d}{d\xi}\right]e_1=-\lambda_{1,1}e_0+p_2-e_2, \tag{138}$$

$$\left[-i\alpha_m+\frac{d}{d\xi}\right]p_1=D_2e_0+D_1e_1-(p_2-e_2). \tag{139}$$

According to Eq. (133), $p_1(\xi)$ can be expressed by

$$p_1=\left[\lambda_{1,0}+\eta_0\frac{d}{d\xi}\right]e_0+e_1. \tag{140}$$

Eliminating (p_2-e_2) by adding Eq. (138) to Eq. (139) and substituting Eq. (140) into Eqs. (138) and (139), we find with some algebra that $e_1(\xi)$ satisfies the following inhomogeneous differential equation:

$$(1+\eta)\frac{de_1}{d\xi}=(i\alpha_m-\lambda_{1,0}+D_1)e_1 + \left[D_2-\lambda_{1,1}+\left[i\alpha_{m-nN}-\frac{D_1}{1+\eta}\right]\times\left[i\alpha_{m-nN}+\frac{\eta D_1}{1+\eta}\right]\right]e_0 . \tag{141}$$

$\lambda_{1,1}$ is determined by the requirement that (e_1,d_2) are periodic functions. Now we refer to the mathematical theorems introduced in Appendix A. Note that the homogeneous part of Eq. (141) is just Eq. (133) and the corresponding adjoint system defined in Appendix A is

$$(1+\eta)\frac{dz}{d\xi}=(i\alpha_m-\lambda_{1,0}-D_1)z , \tag{142}$$

which yields the solution

$$z(\xi)=\exp\left[\frac{i\alpha-\lambda_{1,0}}{1+\eta}\xi-\frac{1}{1+\eta}\int_0^{\xi}D_1(\xi)d\xi\right] . \tag{143}$$

As indicated by Eqs. (134) and (143), $z^*(\xi)e_0(\xi)=\text{const}$. Therefore, according to Theorem II in Appendix A, Eq. (141) has a T-periodic solution if and only if

$$\int_0^T\left[D_2-\lambda_{1,1}+\left[i\alpha_{m-nN}-\frac{D_1}{1+\eta}\right]\times\left[i\alpha_{m-nN}+\frac{\eta D_1}{1+\eta}\right]\right]d\xi=0 . \tag{144}$$

From Eq. (135) it is easy to see that

$$\int_0^T D_1(\xi)d\xi=0 . \tag{145}$$

Therefore, we obtain from Eq. (144) that

$$\lambda_{1,1}=-\alpha_{m-nN}^2+\frac{1}{T}\int_0^T\left[D_2-\frac{\eta D_1^2}{(1+\eta)^2}\right]d\xi . \tag{146}$$

From Eqs. (50) and (51), we can show by straightforward but lengthy calculations that

$$\frac{d^2D_2}{d\xi^2}+\frac{d}{d\xi}\left[D_1-\frac{2D_1D_2}{1+\eta}-\frac{\eta(1-\eta)\Lambda}{2(1+\eta)}\frac{dI_0}{d\xi}+\frac{2\eta^2D_1^3}{3(1+\eta)^3}\right]=\frac{2\Lambda}{1+\eta}\left[\left[\frac{1}{\Lambda}+\frac{\eta^2}{(1+\eta)^2}\right]D_1^2-D_2\right] . \tag{147}$$

The integration of Eq. (147) within a period yields

$$\int_0^T D_2(\xi)d\xi=\left[\frac{1}{\Lambda}+\frac{\eta^2}{(1+\eta)^2}\right]\int_0^T D_1^2(\xi)d\xi . \tag{148}$$

Substituting this expression into Eq. (146), we obtain

$$\lambda_{1,1}=-\alpha_{m-nN}^2+\left[\frac{1}{\Lambda}-\frac{\eta(1-\eta)}{(1+\eta)^2}\right]\frac{1}{T}\int_0^T D_2^2d\xi . \tag{149}$$

Since $\alpha_{m-nN}=0$ for $m=nN$, the Floquet exponent $\lambda_{1,1}$ is nonpositive only if

$$\Lambda\geq\frac{(1+\eta)^2}{\eta(1-\eta)} . \tag{150}$$

As we have mentioned in Sec. II D, the numerical integration shows that Eqs. (55) and (56) have T-periodic solutions $I_1(\xi)$ and $D_2(\xi)$ if and only if the equality in Eq. (150) holds. Thus Eq. (149) becomes

$$\lambda_{1,1}=-\alpha_{m-nN}^2 . \tag{151}$$

We have thus proven that the real part of this Floquet exponent related to (e_-,p_-) is nonpositive. It is interesting to notice that Eq. (151) does not depend on the self-pulsing solutions. The condition $\alpha_{m-nN}=0$ implies that the corresponding perturbations are spatially homogeneous. In comparison to the case of stationary laser solution, the vanishing of this Floquet exponent at $\alpha_{m-nN}=0$ comes from the fact that the self-pulsing solution is independent of the phases of the fields.[1]

D. The Floquet exponent related to (e_+,p_+,d)

Now let us discuss the Floquet exponent Eq. (126) determined by Eqs. (107)–(109). Similar to Eqs. (105) and (106), we obtain the following equations:

$$\sqrt{\gamma}\left[\lambda_1+\eta\frac{d}{d\xi}\right]e_+=p_+-e_+ , \tag{152}$$

$$\sqrt{\gamma}\left[-\alpha_m+\frac{d}{d\xi}\right]p_+=De_+-p_++2Ed , \tag{153}$$

$$\left[-\alpha_m+\frac{d}{d\xi}\right]d=-\sqrt{\gamma}\left[d+\frac{\Lambda}{2}(Ep_++Pe_+)\right] . \tag{154}$$

In order to solve for λ_1, we expand (e_+,p_+,d) into $\sqrt{\gamma}$ series, see Eq. (129). In the zeroth order, we find

$$e_0=p_0,\quad d_0=0 . \tag{155}$$

In the first order, Eqs. (152)–(154) have the form

$$\left[\lambda_{1,0}+\eta\frac{d}{d\xi}\right]e_0=p_1-e_1 , \tag{156}$$

$$\left[-i\alpha_m+\frac{d}{d\xi}\right]p_0=D_1e_0+2E_0d_1-(p_1-e_1) , \tag{157}$$

$$\left[-i\alpha_m+\frac{d}{d\xi}\right]d_1=-\Lambda E_0e_0 . \tag{158}$$

Eliminating (p_1-e_1) by adding Eq. (156) to Eq. (157) and taking Eq. (155) into account, we obtain

$$(1+\eta)\frac{de_0}{d\xi}=(i\alpha_m-\lambda_{1,0}+D_1)e_0+2E_0d_1 . \tag{159}$$

Multiplying on both sides by E_0 and making use of Eq. (19), we may change Eq. (159) into the form

$$(1+\eta)\frac{dE_0e_0}{d\xi}=(i\alpha_m-\lambda_{1,0}+2D_1)E_0e_0+2I_0d_1 . \tag{160}$$

This equation and Eq. (158) form a closed set of equations for $E_0e_0(\xi)$ and $d_1(\xi)$. In general, this set of differential equations can only be solved numerically. In doing so, we find it simpler to introduce the following notations:

$$y_1 \equiv E_0 e_0, \quad y_2 \equiv d_1/\sqrt{(1+\eta)\Lambda}\ , \tag{161}$$

$$\omega_1 \equiv \frac{\alpha_m + i\lambda_{1,0}}{2\sqrt{(1+\eta)\Lambda}}, \quad \omega_2 \equiv \frac{\alpha_m}{2\sqrt{\tilde{\Lambda}}}\ . \tag{162}$$

In terms of $\tilde{\xi}$ and $\tilde{D}_1$ defined in Eqs. (52) and (53) respectively, Eqs. (160) and (158) can be written in the form

$$\frac{d}{d\tilde{\xi}}\begin{bmatrix} y_1 \\ y_2 \end{bmatrix} = \begin{bmatrix} i\omega_1 + \tilde{D}_1 & I_0 \\ -1/2 & i\omega_2 \end{bmatrix}\begin{bmatrix} y_1 \\ y_2 \end{bmatrix}\ . \tag{163}$$

Defining

$$\hat{A} = \begin{bmatrix} i\omega_1 + \tilde{D}_1 & I_0 \\ -1/2 & i\omega_2 \end{bmatrix}\ , \tag{164}$$

Eq. (163) may be simply written as

$$\frac{d\mathbf{y}}{d\tilde{\xi}} = \hat{A}\mathbf{y}\ , \tag{165}$$

where $\mathbf{y} \equiv \binom{y_1}{y_2}$, and $\hat{A}$ is a functional of $I_{\min}$ and $\omega_{1,2}$, because $I_{\min}$ uniquely fixes the functions I_0 and $\tilde{D}$.

In comparison with Eqs. (158) and (160), Eq. (163) or (165) has the advantage that it does not contain Λ, η, and T_s explicitly. Therefore, it can be numerically solved for given parameters $I_{\min}$ (or $I_{\max}$) and $\omega_{1,2}$. For given $I_{\min}$ and ω_2, Eq. (165) has a $\tilde{T}$-periodic solution only for some ω_1. In other words, ω_1, or $\lambda_{1,0}$, is a function of $I_{\min}$ and ω_2. This function will be discussed both analytically and numerically in Secs. V and VI, respectively. The results show that $\lambda_{1,0}$ may be a purely imaginary number or a complex number with a nonvanishing real part, depending on the values of $I_{\min}$ and ω_2.

If $\lambda_{1,0}$ is purely imaginary, we have to calculate $\lambda_{1,1}$ in order to determine the linear stability and the self-pulsing solution. To this end, we study Eqs. (152)–(154) in the order of γ. Similar to Eq. (161), it is convenient to introduce

$$x_1 \equiv E_0 e_1, \quad x_2 \equiv \frac{d_2}{\sqrt{\Lambda(1+\eta)}}\ . \tag{166}$$

By lengthy calculations, which will not be presented here, we obtain the following inhomogeneous equations:

$$\frac{d\mathbf{x}}{d\tilde{\xi}} = \hat{A}\mathbf{x} + \frac{1}{2\sqrt{\tilde{\Lambda}}}\begin{bmatrix} Q_1 - \lambda_{1,1}y_1 \\ Q_2 \end{bmatrix}\ , \tag{167}$$

where $\hat{A}$ is defined in Eq. (164), Q_1 and Q_2 are given by

$$Q_1 = \{\sqrt{\Lambda(1+\eta)}\tilde{D}_2 - \tilde{\Lambda}[4\omega_{21}^2 + 2i\omega_{21}(1-\eta)\tilde{D}_1 + \eta(1+\tilde{D}_1^2 - 3I_0)]\}y_1 + [\sqrt{\Lambda(1+\eta)}I_1 - 4\tilde{\Lambda}I_0(i\omega_{21} + \eta\tilde{D}_1)]y_2\ , \tag{168}$$

$$Q_2 = -\Lambda\left[i\omega_{21} + \eta\tilde{D}_1 + \frac{I_1}{2\sqrt{\tilde{\Lambda}}I_0}\right]y_1 - (1+\eta+\eta\Lambda I_0)y_2\ , \tag{169}$$

where $\omega_{21} \equiv \omega_2 - \omega_1$, and (y_1, y_2) is the periodic solution of Eq. (165).

Our purpose is to find $\lambda_{1,1}$, under the condition that Eq. (167) has a periodic solution. Since the corresponding homogeneous equation, i.e., Eq. (165), has a periodic solution, according to Theorem II(a) in Appendix A, the adjoint system

$$\frac{d\mathbf{z}}{d\tilde{\xi}} = -\hat{A}^*\mathbf{z} \tag{170}$$

also has a periodic solution. Let $\mathbf{z}$ be the periodic solution; then, according to Theorem II(b), we find with some algebra that the inhomogeneous equation (167) has a periodic solution if and only if

$$\langle \mathbf{z}|\mathbf{Q}\rangle - \lambda_{1,1}\langle z_1|y_1\rangle = 0\ , \tag{171}$$

where the operation $\langle\ |\ \rangle$ is defined in Appendix A. Thus, we obtain

$$\lambda_{1,1} = \frac{\langle \mathbf{z}|\mathbf{Q}\rangle}{\langle z_1|y_1\rangle}\ . \tag{172}$$

In the following sections, we shall solve Eqs. (163) and (172). $\lambda_{1,0}$ will be analytically calculated in the small-amplitude limit in Sec. V and both $\lambda_{1,0}$ and $\lambda_{1,1}$ will be numerically computed in Sec. VI for the self-pulsing solutions. The results will show that, in addition to the RNGH-type instability discussed in Sec. III, another kind of instability may occur for the self-pulsing solutions when the oscillating amplitude becomes too large.

V. ANALYTICAL ANALYSIS OF THE FLOQUET EXPONENT $\lambda_{1,0}$ IN THE SMALL-AMPLITUDE LIMIT $I_{\min} \to 1$

In the small-amplitude limit,

$$\delta \equiv 1 - I_{\min} \ll 1\ . \tag{173}$$

Equation (163) can be solved by δ expansion. As we shall show in this section, $\lambda_{1,0}$ may have a positive real part in the order δ^2 if Λ or T_s exceed some critical value. This reveals a new kind of instabilities for the self-pulsing solutions. Our approach is basically a second-order perturbation theory in the degenerate case.

A. Transforming a $\tilde{T}$-periodic solution into a 2π-periodic solution

For small δ, $I_0(\tilde{\xi})$ can be written in the form

$$I_0 = 1 + u(\delta)\delta\ , \tag{174}$$

where $u(\delta)=O(1)$. Using a Taylor expansion, it is easy to show that

$$\ln I_0-\ln I_{\min}+I_{\min}-I_0 = \frac{\delta^2}{2}\left[1+\frac{2\delta}{3}+\frac{\delta^2}{2}\right]\left[1-\frac{u^2(6-4u\delta+3u^2\delta^2)}{6+4\delta+3\delta^2}\right] . \tag{175}$$

Defining

$$s^2\equiv\frac{u^2(6-4u\delta+3u^2\delta^2)}{6+4\delta+3\delta^2} , \tag{176}$$

under the condition $\lim_{\delta\to 0}s=\lim_{\delta\to 0}u$, a straightforward but lengthy calculation yields, to the order δ^2,

$$I_0=1+s\delta+\frac{\delta^2}{3}s(1+s) , \tag{177}$$

$$\sqrt{2}\tilde{D}_1=\pm\delta\left[1+\frac{\delta}{3}\right](1-s^2)^{1/2} , \tag{178}$$

and

$$d\tilde{\xi}=\pm\frac{dI_0}{I_0\sqrt{\ln I_0-\ln I_{\min}+I_{\min}-I_0}} =\pm\left[1-\frac{\delta}{3}s+\frac{\delta^2}{36}s(3s-4)\right]\frac{\sqrt{2}ds}{(1-s^2)^{1/2}} . \tag{179}$$

As is apparent from Eq. (178), to the order δ^2, that I_0 varying in $[I_{\min},I_{\max}]$ corresponds to s varying in $[-1,1]$. Further on, introducing θ by

$$\cos\theta\equiv s,\quad \sin\theta\equiv\mp(1-s^2)^{1/2} , \tag{180}$$

the $\tilde{T}$-periodic functions $I_0(\tilde{\xi})$ and $\tilde{D}_1(\tilde{\xi})$ become 2π-periodic functions of θ

$$I_0=1+\delta\cos\theta+\frac{\delta^2}{3}\cos\theta(1+\cos\theta) , \tag{181}$$

$$\sqrt{2}\tilde{D}_1=-\delta\left[1+\frac{\delta}{3}\right]\sin\theta , \tag{182}$$

$$d\tilde{\xi}=\sqrt{2}\left[1-\frac{\delta}{3}\cos\theta+\frac{\delta^2}{36}\cos\theta(3\cos\theta-4)\right]d\theta . \tag{183}$$

In terms of θ, Eq. (163) takes the form

$$\frac{d\mathbf{y}}{d\theta}=\sqrt{2}\left[1-\frac{\delta}{3}\cos\theta+\frac{\delta^2}{36}\cos\theta(3\cos\theta-4)\right] \times\begin{bmatrix} i\omega_1+\tilde{D}_1 & I_0 \\ -1/2 & i\omega_2\end{bmatrix}\mathbf{y} . \tag{184}$$

Defining

$$Y_1\equiv\frac{y_1}{\sqrt{2}},\quad Y_2\equiv y_2 , \tag{185}$$

$$\beta_1\equiv\sqrt{2}\omega_1,\quad \beta_2\equiv\sqrt{2}\omega_2 , \tag{186}$$

$$\hat{B}\equiv\left[1-\frac{\delta}{3}\cos\theta+\frac{\delta^2}{36}\cos\theta(3\cos\theta-4)\right] \times\begin{bmatrix} i\beta_1+\sqrt{2}\tilde{D}_1 & I_0 \\ -1 & i\beta_1\end{bmatrix} , \tag{187}$$

Equation (184) takes the form

$$\frac{d\mathbf{Y}}{d\theta}=\hat{B}\mathbf{Y} . \tag{188}$$

We shall solve this equation to the order δ^2 and calculate the Floquet exponent $\lambda_{1,0}$. To this end, we expand $\mathbf{Y}$, β_1 and β_2, and $\hat{B}$ into a power series with respect to δ,

$$F(\delta)=F^{(0)}+F^{(1)}\delta+F^{(2)}\delta^2+\cdots , \tag{189}$$

where F may represent $\mathbf{Y}$, β_ν, or $\hat{B}$. Inserting Eq. (189) for $\hat{B}$ into Eq. (187), we obtain

$$\hat{B}^{(0)}=\begin{bmatrix} i\beta_1^{(0)} & 1 \\ -1 & i\beta_2^{(0)}\end{bmatrix} , \tag{190}$$

$$\hat{B}^{(1)}=\begin{bmatrix} i\beta_1^{(1)} & 0 \\ 0 & i\beta_2^{(1)}\end{bmatrix}+\sum_{\epsilon=\pm1}\frac{e^{i\epsilon\theta}}{6}\begin{bmatrix} i(3\epsilon-\beta_1^{(0)}) & 2 \\ 1 & -i\beta_2^{(0)}\end{bmatrix} , \tag{191}$$

$$\hat{B}^{(2)}=\frac{1}{24}\begin{bmatrix} i(\beta_1^{(0)}+24\beta_{1,2}) & 1 \\ -1 & i(\beta_2^{(0)}+24\beta_2^{(2)})\end{bmatrix}+\sum_{\epsilon=\pm1}\frac{e^{i\epsilon\theta}}{18}\begin{bmatrix} i(3\epsilon-\beta_1^{(0)}-3\beta_1^{(1)}) & 2 \\ 1 & -i(\beta_2^{(0)}+3\beta_2^{(1)})\end{bmatrix} +\sum_{\epsilon=\pm1}\frac{\exp 2i\epsilon\theta}{48}\begin{bmatrix} i(\beta_1^{(0)}-4\epsilon) & 1 \\ -1 & -i\beta_2^{(0)}\end{bmatrix} . \tag{192}$$

Equations (191) and (192) can be considered as the Fourier expansions of $\hat{B}^{(1)}$ and $\hat{B}^{(2)}$, respectively, i.e.,

$$\hat{B}^{(1)}=\hat{B}_0^{(1)}+\sum_{\epsilon=\pm1}\hat{B}_\epsilon^{(1)}e^{i\epsilon\theta} , \tag{193}$$

$$\hat{B}^{(2)}+\hat{B}_{2,0}+\sum_{\epsilon=\pm1}\hat{B}_\epsilon^{(2)}e^{i\epsilon\theta}+\sum_{\epsilon=\pm1}\hat{B}_{2\epsilon}^{(2)}e^{2i\epsilon\theta} . \tag{194}$$

The explicit expressions of the Fourier coefficients $\hat{B}_m^{(n)}$ can be easily obtained from Eqs. (191) and (192).

B. The zeroth-order approximation and the degenerate points

In the zeroth order of δ, Eq. (188) is

$$\frac{d}{d\theta}\begin{bmatrix} Y_1^{(0)} \\ Y_2^{(0)}\end{bmatrix}=\begin{bmatrix} i\beta_1^{(0)} & 1 \\ -1 & i\beta_2^{(0)}\end{bmatrix}\begin{bmatrix} Y_1^{(0)} \\ Y_2^{(0)}\end{bmatrix} . \tag{195}$$

The general solution of $Y_1^{(0)}(\theta)$ has the form

$$Y_1^{(0)}=c_1e^{im_1\theta}+c_2e^{im_2\theta}, \tag{196}$$

where c_1 and c_2 are arbitrary constants. Substituting this expression into Eq. (195), we find

$$(\beta_1^{(0)}-m_\nu)(\beta_2^{(0)}-m_\nu)=1 \quad (\nu=1,2), \tag{197}$$

from which it is easy to obtain the following relations:

$$m_\nu=\tfrac{1}{2}\{\beta_1^{(0)}+\beta_2^{(0)}\pm[(\beta_2^{(0)}-\beta_1^{(0)})^2+4]^{1/2}\} \quad (\nu=1,2), \tag{198}$$

$$\beta_{\nu,0}=\tfrac{1}{2}\{m_1+m_2\pm[(m_1-m_2)^2-4]^{1/2}\} \quad (\nu=1,2), \tag{199}$$

$$m_1+m_2=\beta_1^{(0)}+\beta_2^{(0)}. \tag{200}$$

In accord with Eq. (196), $Y_2^{(0)}$ is of the form

$$Y_2^{(0)}=ic_1(m_1-\beta_1^{(0)})e^{im_1\theta}+ic_2(m_2-\beta_1^{(0)})e^{im_2\theta}, \tag{201}$$

and $\mathbf{Y}_0$ is thus given by

$$\mathbf{Y}^{(0)}(\theta)=c_1e^{im_1\theta}\begin{bmatrix}1\\ i(m_1-\beta_1^{(0)})\end{bmatrix}+c_2e^{im_2\theta}\begin{bmatrix}1\\ i(m_2-\beta_1^{(0)})\end{bmatrix}. \tag{202}$$

For $\mathbf{Y}_0(\theta)$ to be 2π periodic, it is necessary that at least one m_ν is an integer, and $c_\nu=0$ if m_ν is not an integer. For convenience, we suppose m_1 to be an integer. From Eq. (197), a given integer m_1 corresponds to a hyperbola in the $(\beta_1^{(0)},\beta_2^{(0)})$ plane. Since m_1 may be an integer, there is an infinity of hyperbolas, each point of which corresponds to a 2π-periodic solution $\mathbf{Y}_0$. As shown in Fig. 6, these hyperbolas form a net which contains tangent points and intersections. Since at these special points both m_1 and m_2 are integers, and hence both c_1 and c_2 may be different from zero, we call them degenerate points, which can be specified by a pair of integers (m_1,m_2). Other points in the net are nondegenerate points.

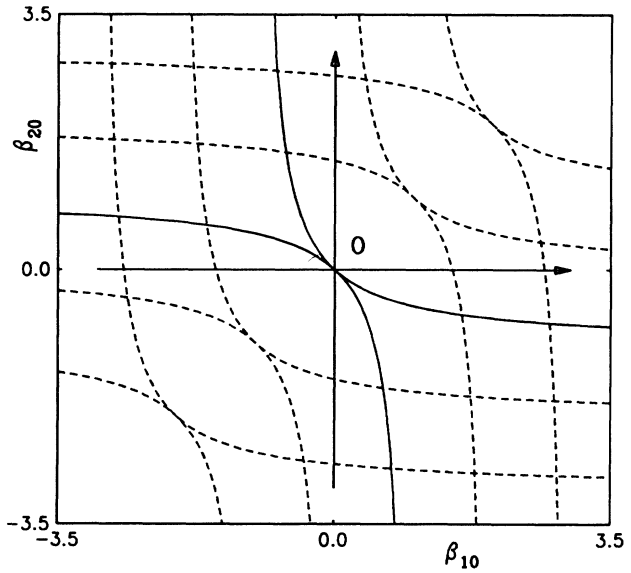

FIG. 6. Graphically illustrated is the net made up of the multivalued function β_1 vs β_2, which contains the degenerate points, i.e., the tangent points and other intersections. For the linear stability analysis it is sufficient to consider β_1 and β_2 on the two solid curves.

As is apparent from Eq. (197), $\beta_1^{(0)}$ is always a real number for real $\beta_2^{(0)}$. This means that $\lambda_{1,0}$ is purely imaginary in the zeroth order of δ. Therefore, in order to analyze the linear stability, we need to calculate the higher-order contributions $\beta_1^{(n)}$ $(n\geq 1)$.

For small δ, we can show that the (β_1,β_2) relation has only a small quantitative deviation from Eq. (197) at the nondegenerate points, but it may qualitatively differ from Eq. (197) at the degenerate points. Here, by qualitative difference we mean that β_1 has an imaginary part. Therefore, we shall focus our attention on the degenerate points.

It is easy to show that all the tangent points in Fig. 6 correspond to $|m_1-m_2|=2$, and all the intersecting points correspond to $|m_1-m_2|\geq 3$. On the other hand, we can show that the largest Fourier index of the evolution operator $\hat{B}^{(n)}$ is n, see Eqs. (191) and (192). Therefore, in order to investigate a degenerate point (m_1,m_2), we need to perform the perturbation theory up to $\delta^{|m_1-m_2|}$. This also means that the $(\beta_1^{(0)},\beta_2^{(0)}$ relation may be qualitatively distorted in the order of $\delta^{|m_1-m_2|}$ of a degenerate point (m_1,m_2). Thus the largest distortion occurs at the tangent points.

Though the net of parabolas shown in Fig. 6 presents a clear picture of the degenerate points, it contains multiplicity. In what follows, we shall show that, in analyzing the linear stability of the self-pulsing solution, all of the pairs of these curves that have different opening directions, including those corresponding to different m_1, are equivalent to each other. In other words, it is sufficient for us to calculate the Floquet exponents for just one pair of the curves in the $(\beta_1^{(0)},\beta_2^{(0)})$.

In fact, by the definitions of β and $\mathbf{Y}$, see Eqs. (89), (99), (161), and (185), the perturbation E_0e_0 in the physical coordinate (ζ,τ) is related to θ in the following way:

$$E_0e_0=\exp\left[\lambda\tau+i\alpha_m\frac{\zeta}{c}\right]Y_1^{(0)}(\theta)$$
$$=\exp\left[\lambda\tau+i\alpha_m\frac{\zeta}{c}+im_1\theta\right]. \tag{203}$$

In the limit $\delta\to 0$, it follows from Eqs. (9), (52), and (183) that

$$\tilde{\xi}\equiv 2\sqrt{\tilde{\Lambda}}\left[\tau-\frac{\zeta}{v}\right]=\sqrt{2}\theta. \tag{204}$$

Substituting this equation for θ into Eq. (203) and taking Eqs. (162) and (186) into account, we can show that

$$E_0 e_0 = \exp\left[\tau\left[\lambda + i\frac{v}{c}\alpha_{m_1} N\right] + i\frac{\alpha_N}{c}\left[\frac{v}{c}\beta_2 - m_1\right]\zeta\right] . \tag{205}$$

This shows that the relevant quantity for the spatial distribution of the perturbation is $(\beta_1^{(0)} - m_1)$, but not $\beta_1^{(0)}$. Therefore, the physical quantity, i.e., the mode parameter, for the stability analysis is $(\beta_1^{(0)} - m_1)$. Obviously, each of the hyperbolas opening upwards satisfies $(\beta_1^{(0)} - m_1) > 0$ and contains all the positive Fourier indexes (cavity modes) and in contrast, each of the hyperbolas opening downwards satisfies $(\beta_1^{(0)} - m_1) < 0$ and contains all the negative Fourier indexes.

Therefore, without loss of generality, we may choose a special pair of the hyperbolas corresponding to $m_1 = \pm 1$ to describe all the cavity modes, see the solid curves in Fig. 6. What is more, since the negative and the positive cavity modes are symmetric, we could consider only one of the solid curves.

In what follows we shall only deal with the tangent point $(\beta_1^{(0)}, \beta_2^{(0)}) = (0,0)$, i.e., $(m_1, m_2) = (-1,1)$ by using the degenerate perturbation theory up to order δ^2.

C. Degenerate perturbation theory at the tangent point

In this case, the zeroth-order solution Eq. (202) takes the form

$$\mathbf{Y}^{(0)}(\theta) = \sum_{\epsilon=\pm 1} c_\epsilon \begin{bmatrix} 1 \\ i\epsilon \end{bmatrix} e^{i\epsilon\theta} = \sum_{\epsilon=\pm 1} \mathbf{Y}_\epsilon^{(0)} e^{i\epsilon\theta} , \tag{206}$$

where we have used $c_{\pm 1}$ instead of $c_{1,2}$ as the arbitrary constants.

In the first order of δ, we obtain from Eq. (188) that

$$\frac{d\mathbf{Y}^{(1)}}{d\theta} = \hat{B}^{(0)}\mathbf{Y}^{(1)} + \hat{B}^{(1)}\mathbf{Y}^{(0)} , \tag{207}$$

where $B_0^{(1)}$ and $B_\epsilon^{(1)}$ are given by

$$\hat{B}_0^{(1)} = \begin{bmatrix} i\beta_1^{(1)} 1 & 0 \\ 0 & i\beta_2^{(1)} \end{bmatrix} , \tag{208}$$

$$\hat{B}_{1,\epsilon} = \frac{1}{6}\begin{bmatrix} 3\epsilon & 2 \\ 1 & 0 \end{bmatrix} . \tag{209}$$

Equation (207) is an inhomogeneous solution for $\mathbf{Y}^{(1)}$. According to Theorem II in Appendix A, it is easy to show that Eq. (207) has a periodic solution if and only if, for $\epsilon = \pm 1$,

$$(\mathbf{Y}_\epsilon^{(0)})^* \hat{B}_0^{(1)} \mathbf{Y}_\epsilon^{(0)} = 0 , \tag{210}$$

which yields

$$\beta_1^{(1)} + \beta_2^{(1)} = 0 . \tag{211}$$

Thus $\hat{B}_0^{(1)}$ takes the form

$$\hat{B}_0^{(1)} = i\beta_1^{(1)}\begin{bmatrix} 1 & 0 \\ 0 & -1 \end{bmatrix} . \tag{212}$$

Substituting Eqs. (206), (209), and (212) into Eq. (207), we obtain

$$\mathbf{Y}^{(1)} = \sum_{\epsilon=\pm 1} c_\epsilon \left[\frac{1}{6}\begin{bmatrix} 1 \\ i\epsilon \end{bmatrix} - i\beta_1^{(1)} e^{i\epsilon\theta}\begin{bmatrix} 0 \\ 1 \end{bmatrix} + \frac{e^{2i\epsilon\theta}}{6}\begin{bmatrix} 3 \\ i\epsilon \end{bmatrix}\right] . \tag{213}$$

To this order, the two zero-order solutions, $Y_\epsilon^{(0)}$ have not been coupled by the perturbations and β_1 remains purely imaginary, just like the case of nondegenerate perturbations.

In the second order, Eq. (188) is

$$\frac{d\mathbf{Y}^{(2)}}{d\theta} = \hat{B}^{(0)}\mathbf{Y}^{(2)} + \hat{B}^{(1)}\mathbf{Y}^{(1)} + \hat{B}^{(2)}\mathbf{Y}^{(0)} . \tag{214}$$

According to Theorem II in Appendix A, for Eq. (2.14) to have a periodic solution, it is necessary that, for $\epsilon = \pm 1$,

$$(\mathbf{Y}_\epsilon^{(0)})^*(\hat{B}_\epsilon^{(1)}\mathbf{Y}_0^{(1)} + \hat{B}_0^{(1)}\mathbf{Y}_\epsilon^{(1)} + \hat{B}_{-\epsilon}^{(1)}\mathbf{Y}_{2\epsilon}^{(1)} + \hat{B}_0^{(2)}\mathbf{Y}_\epsilon^{(0)} + \hat{B}_{2\epsilon}^{(2)}\mathbf{Y}_{-\epsilon}^{(0)}) = 0 . \tag{215}$$

Making use of Eqs. (192) and (211), and taking $(\beta_1^{(0)}, \beta_2^{(0)}) = (0,0)$ and $m_\epsilon = \epsilon$ into account, we find from Eq. (215) the following two equations:

$$\beta_1^{(2)} + \beta_2^{(2)} + \frac{1}{12} + \frac{c_+}{12c_-} - (\beta_1^{(1)})^2 = 0 , \tag{216}$$

$$\beta_1^{(2)} + \beta_2^{(2)} - \frac{1}{12} - \frac{c_-}{12c_+} + (\beta_1^{(1)})^2 = 0 , \tag{217}$$

which yields

$$\beta_1^{(2)} + \beta_2^{(2)} = \pm\beta_2^{(1)}[(\beta_2^{(1)})^2 - \tfrac{1}{6}]^{1/2} , \tag{218}$$

$$\frac{c_+}{c_-} = -1 + 12(\beta_2^{(1)})^2 \mp [(\beta_2^{(1)})^2 - \tfrac{1}{6}]^{1/2} . \tag{219}$$

Equation (218) shows that $\beta_1^{(2)}$ is imaginary if $0 < |\beta_2^{(1)}| < 1/\sqrt{6}$. Equation (219) shows that, to make $\mathbf{Y}^{(2)}$ a periodic solution, the c_ϵ must be related to each other. This relation is useful for calculating $\lambda_{1,1}$ at the tangent point, which will not be discussed in this paper. β_1 versus β_2 in the cases of $\delta = 0$ and $\delta \neq 0$ is illustrated in Fig. 7.

Since $\beta_2^{(1)}$ is a free parameter, we may put $\beta_2^{(2)} = 0$. Then, from the definitions, Eqs. (162) and (186), we obtain in the vicinity of $(\beta_1^{(0)}, \beta_2^{(0)}) = (0,0)$

$$\lambda_{1,0} = i\sqrt{2\tilde{\Lambda}}\beta_2^{(1)}\delta\{\eta \pm (1+\eta)\delta[(\beta_2^{(1)})^2 - \tfrac{1}{6}]^{1/2}\} . \tag{220}$$

Obviously, $\lambda_{1,0}$ may have a positive real part if

$$0 < |\beta^{(1)}| < 1/\sqrt{6} , \tag{221}$$

which in terms of the physical quantities can be expressed as

$$\left|\frac{2\pi n}{T_s}\right| < \delta\frac{\sqrt{\tilde{\Lambda}}}{3} , \tag{222}$$

where n is the cavity mode index. Obviously, the first unstable mode index is $n = 1$. Therefore, in the case of Eq. (173), the self-pulsing solution is unstable if

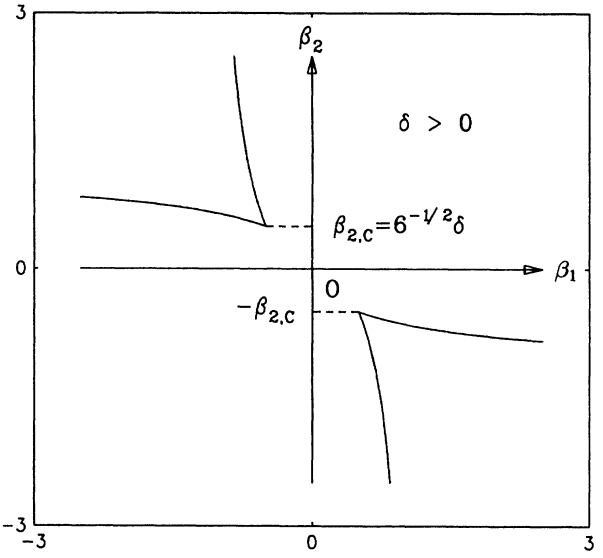

FIG. 7. For $\delta > 0$, β_1 is real only if $|\beta_2| > \beta_{2,C}$.

$$\frac{2\pi}{T_s} < \delta \frac{\sqrt{\tilde{\Lambda}}}{3} . \tag{223}$$

This unstable region is shown in Fig. 8. In the limit $T_s \equiv \sqrt{\gamma_\parallel \gamma_\perp} L/c \to \infty$, this inequality always holds and hence the self-pulsing solution is unstable. For finite T_s, Eq. (223) may be satisfied for sufficiently large pump $\tilde{\Lambda}$. However, in the latter case, δ will become finite and hence the δ expansion will break down. Nevertheless, Eq. (223) suggests that the unstable region becomes larger with $\tilde{\Lambda}$, i.e., the self-pulsing will become unstable if its amplitude is too large. This idea is supported by the numerical calculations presented in Sec. VI.

VI. NUMERICAL CALCULATIONS OF THE FLOQUET EXPONENT

We have shown, in the limits $\chi, \gamma \to 0$, that among the five Floquet exponents only one of them may possess a real part. This Floquet exponent has the form

$$\lambda = -i\alpha_m + \lambda_{1,0}\chi + \lambda_{1,1}\chi\gamma + \cdots . \tag{224}$$

In Sec. V, concerning the small-amplitude limit, we have analytically calculated $\lambda_{1,0}$, and the results reveal a new kind of instability, which may occur if the cavity is sufficiently long or the pump is sufficiently large. Though $\lambda_{1,1}$ has not been calculated, the relation between the RNGH instability and the self-pulsing solutions found in Sec. III provides a description of $\lambda_{1,1}$ in the small-amplitude limit.

In this section, $\lambda_{1,0}$ and $\lambda_{1,1}$ will be numerically computed for arbitrary oscillating amplitudes. Similar to the small-amplitude case, we can show that, though ω_1 is a multivalued function of ω_2, in order to analyze the linear stability it is sufficient to consider one branch of this function, and we shall discuss the same branch illustrated by the solid curves in Fig. 6. As we shall see, $\lambda_{1,0}$ is responsible for the so-called large-amplitude instability, while $\lambda_{1,1}$ describes the RNGH-type instability. Obviously, the characteristic time scale for the large-amplitude instability is $(\sqrt{\gamma_\parallel \gamma_\perp}\chi)^{-1}$, and for the RNGH-type instability it is $(\sqrt{\gamma_\parallel \gamma_\perp \chi\gamma})^{-1}$.

A. Results about $\lambda_{1,0}$ and the large-amplitude instability

The general behavior of $\lambda_{1,0}$ as a function of the cavity mode ω is similar to that in the small-amplitude case, see Sec. V and Figs. 6–8.

In order to find the instability threshold, we first take ω_2 as a continuous parameter. Numerical calculations show that there exists a critical value ω_c for given $I_{\max}$.

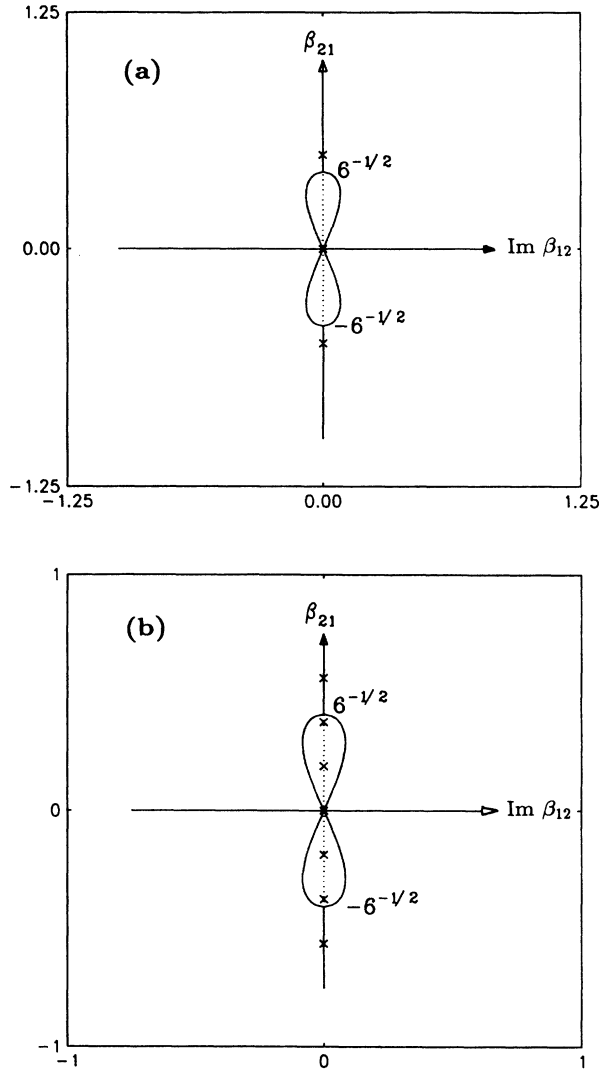

FIG. 8. For $0 < |\beta_{21}| < 1/\sqrt{6}$, there are two purely imaginary solutions for β_{12} and one of them leads to $\mathrm{Re}\lambda_{1,0} > 0$. (a) If no cavity modes are located in the unstable region marked by the dotted line, the instability will not occur; (b) if some cavity modes fall into the unstable region, the self-pulsing solution is unstable.

If $|\omega_2| > \omega_c$, then ω_1 is a real number and hence $\lambda_{1,0}$ is purely imaginary; if $0 < |\omega_2| < \omega_c$, then there are a pair of mutually complex conjugate solutions ω_1, one of which leads to a positive real part of $\lambda_{1,0}$, just like the relations between β_1 and β_2, as shown in Fig. 8.

Since only $I_{\min}$ or $I_{\max}$ is involved in Eq. (163), ω_c is a function of $I_{\max}$ or $I_{\min}$. This function can be numerically computed and the result is shown in Fig. 9. We see that $\omega_c(I_{\max})$ first increases with $I_{\max}$ and then decreases with it. The physical meaning of this behavior will be discussed later.

For a laser with finite cavity length, only discrete values of ω_2 are allowed. Therefore, $\lambda_{1,0}$ has a positive real part if the least nonzero ω_2 satisfies $|\omega_2| < \omega_c$.

In order to find the corresponding instability threshold, let us introduce

$$S \equiv \frac{1}{\sqrt{2\pi}} \int_{I_{\min}}^{I_{\max}} \frac{dy}{\sqrt{\ln y - \ln I_{\min} + I_{\min} - y}} = \frac{T_s \sqrt{\tilde{\Lambda}}}{\sqrt{2N\pi}} , \tag{225}$$

where the second equality comes from Eq. (41). Since there exists a one-to-one correspondence between S and $I_{\min}$, ω_c is a function of S, i.e., $\omega_c = \omega_c(S)$, where $S \geq 1$ according to Eq. (82).

By means of Eq. (162), the least nonzero $|\omega_2|$ corresponds to $\alpha_1 = 2\pi/T_s$, i.e.,

$$\omega_{2,\min} = \frac{\pi}{T_s \sqrt{\tilde{\Lambda}}} . \tag{226}$$

Therefore, for a self-pulsing solution to be stable it is necessary that

$$\frac{\pi}{T_s \sqrt{\tilde{\Lambda}}} > \omega_c . \tag{227}$$

In terms of S, this condition can be written as

$$S\omega_c(S) < \frac{1}{\sqrt{2N}} . \tag{228}$$

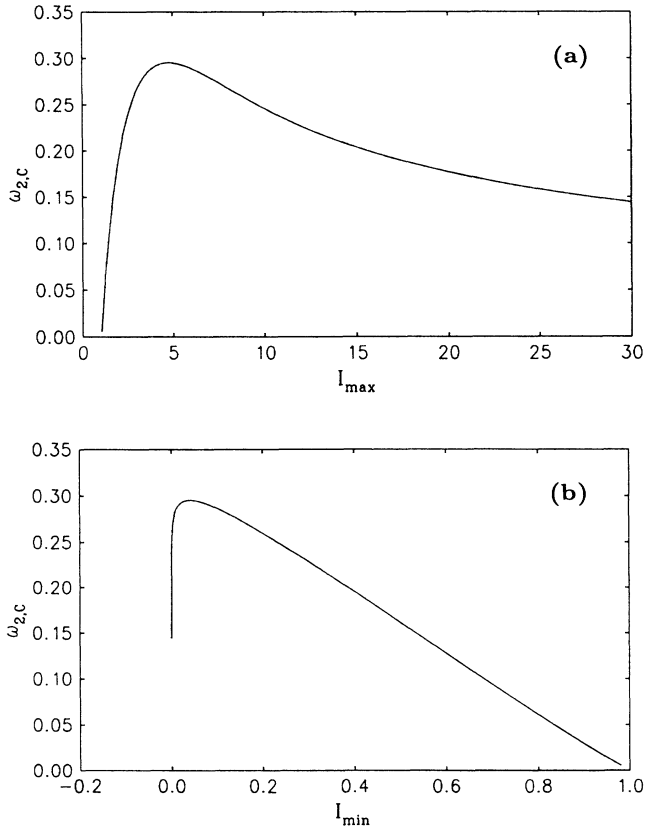

FIG. 9. $\omega_{2,C}$ as a function of $I_{\max}$ and $I_{\min}$.

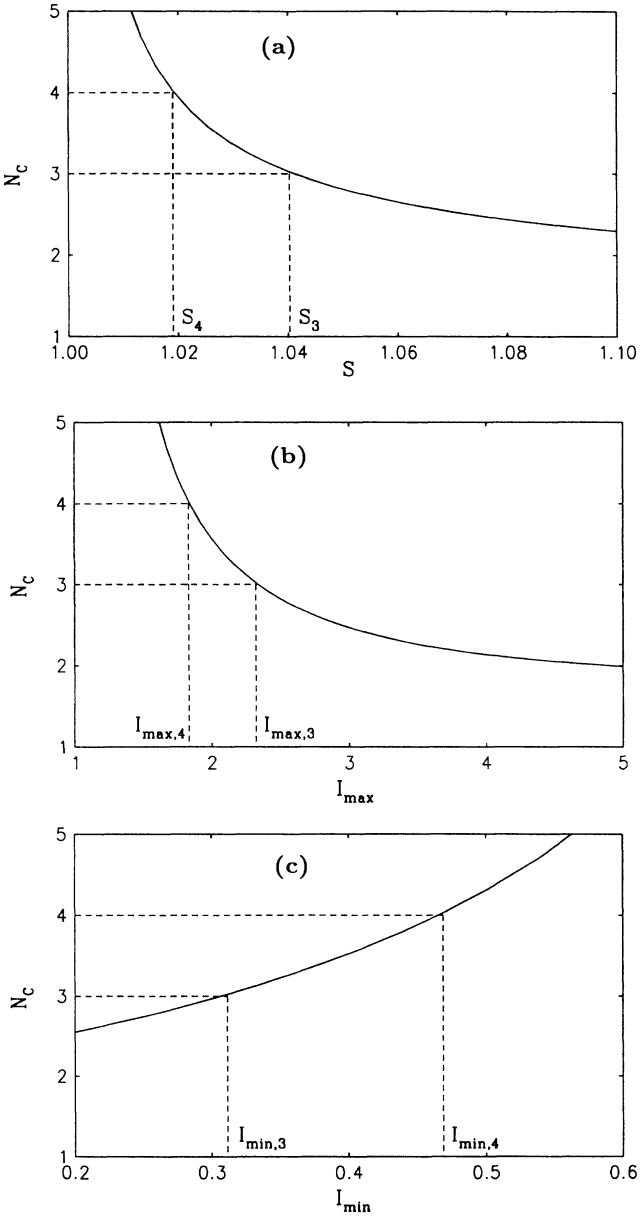

FIG. 10. N_C as a function of S, $I_{\max}$, and $I_{\min}$, and the definitions of S_N, $I_{\max,N}$, and $I_{\min,N}$. An N-pulse self-pulsing solution is stable only if one of the following inequalities holds, namely, $S < S_N$, $I_{\max} < I_{\max,N}$, or $I_{\min} > I_{\min,N}$.

Numerical calculations show that, by increasing S, the left-hand side will exceed the right-hand side at some critical value provided $N \geq 2$, see Fig. 10. To describe this critical value we introduce S_N,

$$S_N \omega_c(S_N) = \frac{1}{\sqrt{2N}}, \quad N \geq 2 , \tag{229}$$

which depends only on N and is a system-independent quantity. Thus, the stability condition Eq. (227) reads

$$S = \frac{\pi}{T_s \sqrt{\tilde{\Lambda}}} < S_N, \quad N \geq 2 . \tag{230}$$

The system-independent threshold values of $S_2, \ldots, S_{20}$, and the corresponding amplitudes of $I_{\min}$ and $I_{\max}$ are listed in Table I. For a given N-pulse self-pulsing, the instability occurs if $S > S_N$, $I_{\min} < I_{\min,N}$, or $I_{\max} > I_{\max,N}$. Since this instability occurs when the oscillating amplitude of the self-pulsing solution is sufficiently large, we call it large-amplitude instability, in contrast to the RNGH-type instability discussed in Sec. III.

The values listed in Table I show that

$$NS_N < N + 1 . \tag{231}$$

This results means that the large-amplitude stability occurs before a second mode entering the RNGH-instability domain shown in Fig. 4. It is easy to show (the proof will not be given here) that the self-pulsing solution that we have found consists of one basic frequency component, which corresponds to the mode α_{RNGH} and its harmonics. Therefore, such a self-pulsing solution must become unstable when another mode with different basic frequency is excited at higher pump parameters.

TABLE I. System-independent threshold values of S_N, $N = 2$–20, and the corresponding amplitudes of $I_{\min}$ and $I_{\max}$.

N	S_N	$I_{\min,N}$	$I_{\max,N}$
2	1.197 415	0.074 647 2	4.913 885
3	1.041 128	0.306 495 5	2.338 600
4	1.019 303	0.465 209 8	1.840 531
5	1.011 428	0.564 072 1	1.617 571
6	1.007 618	0.631 543 6	1.489 720
7	1.005 463	0.680 639 9	1.406 383
8	1.004 120	0.718 028 9	1.347 598
9	1.003 222	0.747 490 9	1.303 831
10	1.002 592	0.771 325 1	1.269 940
11	1.002 131	0.791 013 9	1.242 905
12	1.001 785	0.807 559 2	1.220 825
13	1.001 517	0.821 662 1	1.202 446
14	1.001 306	0.833 829 0	1.186 905
15	1.001 136	0.844 434 4	1.173 590
16	1.000 998	0.853 762 2	1.162 053
17	1.000 884	0.862 030 7	1.151 959
18	1.000 788	0.869 411 4	1.143 053
19	1.000 708	0.876 040 3	1.135 136
20	1.000 639	0.882 027 0	1.128 051

Having found S_N, we can solve Eq. (232) and obtain the threshold of the large-amplitude instability

$$\tilde{\Lambda}_{N,C} \equiv 2 \left[\frac{\pi N S_N}{T_s} \right]^2 , \tag{232}$$

which yields the critical pump $\Lambda_{N,C}$,

$$\Lambda_{N,C} = \tfrac{1}{2}[3\tilde{\Lambda}_{N,C} - 1 - (1 - 6\tilde{\Lambda}_{N,C} + \tilde{\Lambda}_{N,C}^2)^{1/2}] . \tag{233}$$

A multipulse self-pulsing solution is stable only if $\Lambda < \Lambda_{N,C}$. When $\Lambda > \Lambda_{N,C}$, the perturbation with the mode $\exp(i 2\pi\zeta / T_s)$ will grow and the self-pulsing solution will become unstable.

For the single-pulse self-pulsing solution, the large-amplitude instability appears in a different way. In this case, the above-mentioned unstable modes $\alpha_{\pm 1}$ are just the self-pulsing solution itself which has already grown up. In other words, the perturbation of such modes will not grow. This is reflected by the fact that ω_c decreases with $I_{\max}$ for large $I_{\max}$ so that the inequality Eq. (228) always holds for $N = 1$. Therefore, the instability must be caused by other cavity modes, which will not be discussed in this paper.

B. Results about $\lambda_{1,1}$ and the RNGH-type instability

Though the numerical calculation of $\lambda_{1,1}$ involves complicated procedures, the final results are just an extension of the conclusions that we have arrived at in Sec. III, i.e., the instability described by $\lambda_{1,1}$ belongs to the RNGH-type instability. In fact, in all of our calculations concerning various parameters, we find that the sign of the real part of $\lambda_{1,1}$ does not depend on the amplitude of the self-pulsing solution.

It is worth pointing out that $\lambda_{1,1}$ cannot be determined by Eq. (172) at the point $(\omega_1, \omega_2) = (0,0)$, because Eq. (171) becomes an identity for any $\lambda_{1,1}$. At this point, $\lambda_{1,1}$ can only be determined by the higher-order approximations with respect to γ. However, according to the general theory about the stability of periodic solutions, there must be a zero Floquet exponent which corresponds to the perturbation moving along the same direction as the periodic solution in the phase space. Therefore, in addition to the zero exponent discussed in Sec. IV C, which results from the indetermination of the phase of the electric field, there must be another zero Floquet exponent. Since the three exponents discussed in Sec. IV B differ from zero, the remaining zero Floquet exponent must identify itself with this $\lambda_{1,1}$. Some examples of $\lambda_{1,1}$ versus the discrete cavity mode number m are shown in Fig. 11.

It is worth pointing out the reason why we cannot show in the linear stability analysis that the subcritical η_+ solution, as illustrated in Fig. 5(b), is unstable. In fact, since this instability should be caused by the attraction of the stationary solution, it corresponds to a perturbation mode $m = N$, where N is the pulse number of the self-pulsing. According to Eq. (205), this mode corresponds to $\omega_2 = 0$, which always leads to a vanishing Floquet exponent.

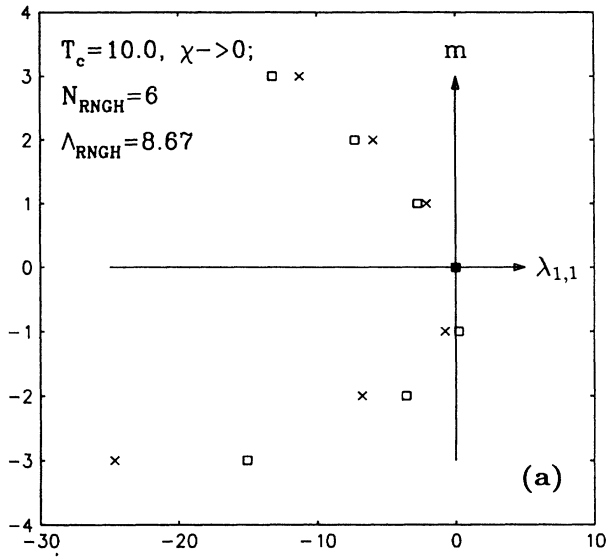

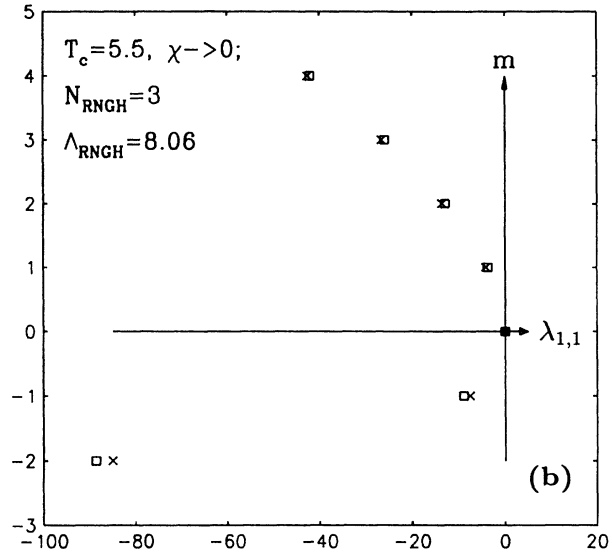

FIG. 11. (a) $\lambda_{1,1}$ vs mode index m for self-pulsing solutions corresponding to the RNGH intersection (crosses) and to non-RNGH intersection (squares) in the case where the RNGH intersection lies in the upper boundary of the RNGH unstable region. The $N=N_{\mathrm{RNGH}}=6$ solution is stable for $\Lambda_{\mathrm{RNGH}}<\Lambda<\Lambda_{N,C}$ as described by the crosses, which is calculated at a particular value $\Lambda=8.72$. The self-pulsing solution corresponding to the non-RNGH intersection with $N=7$ is unstable, as described by the squares, which is calculated at $\Lambda=11.0$. (b) $\lambda_{1,1}$ vs mode index m for the self-pulsing solutions corresponding to $\eta=\eta_-$ (crosses) and to $\eta=\eta_+$ (squares), in the case where the RNGH intersection lies in the lower boundary of the RNGH unstable region, and $N=N_{\mathrm{RNGH}}=3$ and $\Lambda=8.05$. In the linear analysis, we cannot prove that the η_+ solution is unstable; for details see text.

VII. RELATIONS BETWEEN THE SELF-PULSING SOLUTIONS AND THE LORENZ MODEL

By means of the transformation

$$P_r\equiv\frac{1}{\eta},\quad b\equiv\gamma,\quad r\equiv 1+\Lambda\ . \tag{234}$$

Graham showed that Eqs. (11)–(13) are equivalent to the Lorenz equation,[10]

$$\dot{X}=-P_r(X-Y),\quad \dot{Y}=-XZ+rX-Y,\quad \dot{Z}=XY-bZ\ , \tag{235}$$

where X,Y,Z corresponds to E,P,D, respectively, and the dots indicate differentiation with respect to the local time ξ. Therefore, the self-pulsing solutions presented in the preceding sections are also solutions of the Lorenz model in the small-b limit. In addition, the function $\eta_{\pm}(\Lambda)$ as given by Eq. (66) turns out to be the critical boundary of the Lorenz instability

$$r=r_c=\frac{P_r(P_r+b+3)}{P_r-b-1} \tag{236}$$

in the limit $b\to 0$. Figure 12 shows this critical boundary for given b in the (P_r,r) plane. The left-hand side of the boundary is given by $\eta=\eta_+$, which corresponds to unstable or unphysical self-pulsing solutions; the right-hand side is given by $\eta=\eta_-$, which corresponds to the stable self-pulsing solutions under certain conditions.

Since the self-pulsing solutions are always confined within this boundary, we conclude that the traveling-wave self-pulsing solution occurring in a multimode laser system does not correspond to the subcritical solutions of the Lorenz model, as suggested in Ref. 10.

Though our discussions are based on the limit $b=\gamma\to 0$, the conclusion that the periodic self-pulsing solutions of Eqs. (11)–(13) are confined in the unstable boundary equation (236) may be generalized to arbitrary $b=\gamma$. This postulate is equivalent to that expressed by Eq. (83), which describes the relation between the RNGH

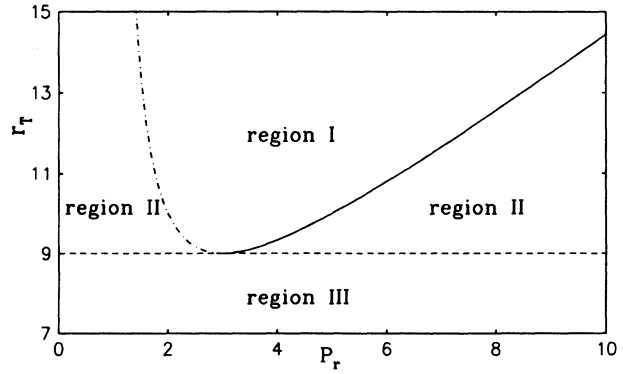

FIG. 12. Threshold condition of the Lorenz instability in the (P_r,r) plane, see Ref. 10. A stable self-pulsing solution may appear for parameters belonging to the right-hand side of the boundary as illustrated by the solid curve.

instability and the self-pulsing solutions. If this is true, then Eq. (66) is just a special case of Eq. (236), which yields the solution

$$\eta_{\pm}=\frac{-2-\gamma+\Lambda\pm[\Lambda^2-(8+6\gamma)\Lambda+\gamma^2]^{1/2}}{2(1+\gamma)(1+\Lambda)} . \quad (237)$$

Therefore, the difficulties of finding the self-pulsing solutions which have space- and time-independent phase velocity for general system equations (11) and (12) will be reduced. For example, as mentioned in Sec. II C, η_1, as defined in Eq. (14), cannot be determined by the perturbation theory up to the order γ, but according to Eq. (237), we find easily that $\eta_1=0$.

VIII. SUMMARY AND CONCLUSIONS

The basic goal of this paper has been to present the analytical self-pulsing solutions arising from the RNGH instability, to establish the correspondence between the self-pulsing and the RNGH instability, and to investigate the instabilities of the self-pulsing solutions. The analytical self-pulsing solutions are presented in Sec. II C in an implicit form.

By linear stability analysis based on the full set of Maxwell-Bloch equations, we have found that two kinds of instabilities may occur for the self-pulsing solutions, namely, the RNGH-type instabilities and the large-amplitude instabilities. The physical origin of the RNGH-type instability lies in that the corresponding self-pulsing solution does not contain the cavity mode which has been excited above the second threshold Λ_{RNGH}. The large-amplitude instability occurs when more than one mode of different basic frequencies are excited. In this case, no stable traveling-wave self-pulsing solution exists and the phase velocity must become space and time dependent. For the moment, we do not know whether and how the large-amplitude instability would lead to the breathing phenomena or the other complicated phenomena, which have been revealed numerically in Refs. 11, 24, and 25.

Considering the two kinds of instabilities, we have shown the following results.

(1) If the RNGH unstable mode lies on the upper boundary of the RNGH-instability region, the N_{RNGH} self-pulsing solution is supercritical and is stable for $\Lambda_{\mathrm{RNGH}}<\Lambda<\Lambda_{N_{\mathrm{RNGH}},C}$ and the $N_{\mathrm{RNGH}}-1$ solution can also be stable in the region $\Lambda_{2\mathrm{nd}}<\Lambda<\Lambda_{N_{\mathrm{RNGH}}-1,C}$ if $\Lambda_{2\mathrm{nd}}<\Lambda_{N_{\mathrm{RNGH}}-1,C}$.

(2) For the unstable mode in the lower boundary, if $I_{\max}<I_{\max,N_{\mathrm{RNGH}}}$ at $\Lambda=\Lambda_{2\mathrm{nd}}$, then the subcritical N_{RNGH} self-pulsing arises for $\Lambda_{2\mathrm{nd}}<\Lambda<\Lambda_{N_{\mathrm{RNGH}},C}$ and the system is bistable; if $I_{\max}>I_{\max,N_{\mathrm{RNGH}}}$ at $\Lambda=\Lambda_{2\mathrm{nd}}$, there is no stable traveling-wave self-pulsing solution at all.

Since there have been no definite experimental results for the RNGH instabilities and the corresponding self-pulsings up to now,[19] this simple rule provides new signatures of the self-pulsing phenomena and will be helpful to experimental identification of the self-pulsing arising from the RNGH instability.

Though our work is based on the limit $\gamma\to 0$, it sheds some light on the general case where γ may be any finite positive number and provides insight into the self-pulsing phenomena. It is worth pointing out that the linear stability analysis does not provide information about the stability when the Floquet exponent is equal to zero, as we encountered in calculating the two relevant Floquet exponents for the spatially homogeneous perturbations. In this case, one has to go to the nonlinear regime of perturbations.

ACKNOWLEDGMENTS

We thank L. A. Lugiato and L. M. Narducci for helpful discussions and for sending us relevant reprints. We also wish to thank D. J. Biswas, R. Friedlich, G. Hu, J.-L. Luo, and C.-Z. Ning for helpful discussions, and M. Bestehorn, A. Fuchs, B. Hölle, A. Hübler, and T. Kuhn for their general assistance in using the computer systems. This research was supported in part by the Volkswagenwerk Foundation, Hannover.

APPENDIX A: TWO THEOREMS ABOUT THE LINEAR DIFFERENTIAL EQUATIONS WITH PERIODIC COEFFICIENTS

In our discussions, the following two theorems concerning a linear differential equation with periodic coefficients are useful, see. Ref. 41.

Let us first consider a homogeneous differential equation

$$\frac{d\mathbf{y}}{dt}=\hat{A}\mathbf{y} , \quad (A1)$$

where $\hat{A}$ is a T-periodic matrix

$$\hat{A}(t+T)=\hat{A}(t) . \quad (A2)$$

Define the matrix $\hat{Y}(t)$ to describe the solutions of Eq. (A1) by

$$\frac{d\hat{Y}}{dt}=\hat{A}\hat{Y},\quad \hat{Y}(0)=\hat{I} . \quad (A3)$$

where $\hat{I}$ is the unit matrix. For this system, we have the following.

Theorem I. Equation (A1) has T-periodic solutions if and only if

$$\det[\hat{Y}(T)-\hat{I}]=0 , \quad (A4)$$

and when Eq. (A4) is satisfied, the initial value of the T-periodic solution $\mathbf{y}(t)$ satisfies

$$\hat{Y}(T)\mathbf{y}(0)=\mathbf{y}(0) . \quad (A5)$$

Now let us consider an inhomogeneous linear differential system

$$\frac{d\mathbf{x}}{dt}=\hat{A}\mathbf{x}+\mathbf{f} , \quad (A6)$$

where $\hat{A}(t)$ satisfies Eq. (A2) and $\mathbf{f}(t)$ satisfies

$$\mathbf{f}(t+T)=\mathbf{f}(t) . \quad (A7)$$

In our discussions, only the case that the corresponding homogeneous system

$$\frac{d\mathbf{y}}{dt}=\hat{A}\mathbf{y} \tag{A8}$$

has d ($d\geq 1$) linearly independent T-periodic solutions is concerned.

Define the adjoint system of Eq. (A8) by

$$\frac{d\mathbf{z}}{dt}=-\hat{A}^{*}\mathbf{z}\ . \tag{A9}$$

Then, we have the following.

Theorem II. (a) The adjoint system Eq. (A9) also has d T-periodic solutions $\mathbf{z}_1,\mathbf{z}_2,\ldots,\mathbf{z}_d$ which satisfy the initial condition

$$\hat{Y}^{*}(T)\mathbf{z}_k(0)=\mathbf{z}_k(0)\quad (k=1,2,\ldots,d)\ . \tag{A10}$$

(b) The inhomogeneous equation, Eq. (A6), has T-periodic solutions if and only if

$$\langle \mathbf{z}_k|\mathbf{f}\rangle=0\quad (k=1,2,\ldots,d)\ , \tag{A11}$$

where, for n-dimension vectors $\mathbf{z}$ and $\mathbf{f}$, $\langle \mathbf{z}|\mathbf{f}\rangle$ means

$$\langle \mathbf{z}|\mathbf{f}\rangle\equiv\frac{1}{T}\int_0^T\left[\sum_{l=1}^{n}f_l^{*}(t)z_l(t)\right]dt\ . \tag{A12}$$

Numerically, in order to find the T-periodic solution of Eq. (A6) satisfying Eq. (A11), we still need to know the initial values of the periodic solution. In what follows, we only discuss a special two-dimensional case which is encountered in solving $I_1(\xi)$ and $D_2(\xi)$.

Assuming that $\mathbf{z}_1(t)$ is a T-periodic function of the adjoint system Eq. (A9) satisfying Eq. (A11) and the initial condition

$$\mathbf{z}_1(0)=\begin{bmatrix}1\\0\end{bmatrix}\ . \tag{A13}$$

Assume $\mathbf{z}_2(t)$ is another solution of Eq. (A9) satisfying

$$\mathbf{z}_2(0)=\begin{bmatrix}0\\1\end{bmatrix},\quad \mathbf{z}_2(T)=\begin{bmatrix}z_{21}\\1\end{bmatrix}\ , \tag{A14}$$

where $z_{21}\neq 0$, i.e., $\mathbf{z}_2$ is not a T-periodic solution. Then, according to Ref. 41, the T-periodic solution $\mathbf{x}(t)$ of Eq. (A6) satisfies the initial condition

$$[\mathbf{z}_2(T)-\mathbf{z}_2(0)]^{*}\mathbf{x}(0)=\langle \mathbf{z}_2|\mathbf{f}\rangle \tag{A15}$$

or

$$\mathbf{x}(0)=\begin{bmatrix}\langle \mathbf{z}_2|\mathbf{f}\rangle/z_{21}^{*}\\ \text{const}\end{bmatrix}\ , \tag{A16}$$

where const is an arbitrary constant, resulting from the fact that a T-periodic solution of the inhomogeneous system plus a T-periodic solution of the corresponding homogeneous system is also a T-periodic solution of the original inhomogeneous system.

APPENDIX B: RESULTS AND EXPRESSIONS FOR $\eta_1\neq 0$

Listed below are the resulting equations containing the parameter η_1, which has been put to zero in the main text. In accord with Eq. (55), the complete differential equation for the first-order intensity I_1 is

$$\frac{dI_1}{d\tilde{\xi}}=D_1I_1+I_0\tilde{D}_2-\frac{\eta_0\sqrt{\tilde{\Lambda}}}{1+\eta_0}I_0(\tilde{D}_1^{\,2}+1-I_0)-\frac{\eta_1I_0\tilde{D}_1}{1+\eta_0}\ . \tag{B1}$$

Equation (56) remains unchanged.

Based on this equation and Eq. (56), we can show that the periodicity condition, Eq. (65), does not change. Therefore, η_0 as a function of Λ is still given by Eq. (66). The zeroth-order Floquet exponents $\lambda_{1,0}$ as discussed in Sec. IV are independent of $\eta_{1,0}$. The first-order term $\lambda_{1,1}$ given by Eq. (151) in the case of $\eta_1\neq 0$ becomes

$$\lambda_{1,1}=-i\eta_1\alpha_{m-Nn}-\alpha_{m-nN}^2\ . \tag{B2}$$

Obviously, the real part is not changed.

In order to calculate the relevant Floquet exponent $\lambda_{1,1}$ as discussed in Sec. IV D, we need to solve I_0, I_1, $\tilde{D}_1$, $\tilde{D}_2$, $\mathbf{y}$, and $\mathbf{z}$ and then find $\tilde{Q}_1$ and $\tilde{Q}_2$. For $\eta_1\neq 0$, I_1 should satisfy Eq. (B1) and $\tilde{Q}_1$ is given by

$$\begin{aligned}\tilde{Q}_1=\{&[\Lambda(1+\eta_0)]^{1/2}\tilde{D}_2-\tilde{\Lambda}[4\omega_{21}^2+2i\omega_{21}(1-\eta_0)\tilde{D}_1\\&+\eta_0(1+\tilde{D}_1^2-3I_0)]\}y_1\\&+\{[\Lambda(1+\eta_0)]^{1/2}I_1-4\tilde{\Lambda}I_0(i\omega_{21}+\eta_0\tilde{D}_1)\}y_2\\&-2\sqrt{\tilde{\Lambda}}\eta_1(\tilde{D}_1y_1+I_0y_2)\ ,\end{aligned} \tag{B3}$$

and the other quantities are determined by the same equations given in the main text. Numerical calculations show that η_1 does not contribute to the real part of the Floquet exponent $\lambda_{1,1}$ determined by Eq. (172). Therefore, we conclude that, up to the order γ, η_1 is irrelevant to the self-pulsing solutions and their linear stability.

[1] H. Risken and K. Nummedal, J. Appl. Phys. **39**, 4662 (1968).
[2] R. Graham and H. Haken, Z. Phys. **213**, 420 (1968).
[3] H. Haken, Z. Phys. B **21**, 105 (1975).
[4] H. Haken and H. Ohno, Opt. Commun. **16**, 205 (1976).
[5] H. Ohno and H. Haken, Phys. Lett. **59A**, 261 (1976).
[6] H. Haken and H. Ohno, Opt. Commun. **26**, 117 (1976).
[7] H. Haken, *Synergetics—An Introduction*, 3rd ed. (Springer-Verlag, Berlin, 1983).
[8] H. Haken, *Advanced Synergetics* (Springer-Verlag, Berlin, 1987).
[9] H. Haken, Phys. Lett. **53A**, 77 (1975).
[10] R. Graham, Phys. Lett. **58A**, 440 (1976).
[11] M. Mayr, H. Risken, and H. D. Vollmer, Opt. Commun. **36**, 480 (1981).
[12] P. W. Smith, M. A. Duguay, and E. P. Ippen, Prog. Quantum Electron. **3**,107 (1975).
[13] G. H. C. New, Rep. Prog. Phys. **46**, 877 (1983).
[14] J. Opt. Soc. Am. B, special issue, **2** (1985).
[15] R. Harrison and D. J. Biswas, Prog. Quantum Electron **10**, 3 (1985).

[16]*Optical Instabilities, Proceedings of the International Meeting on Instabilities and Dynamics of Lasers and Nonlinear Optical Systems,* edited by R. W. Boyd, M. G. Raymer, and L. M. Narducci (Cambridge University Press, Cambridge, England, 1986).

[17]P. W. Milonni, M. L. Shih, and J. R. Ackerhalt, *Chaos in Laser-Matter Interactions* (World Scientific, Singapore, 1987).

[18]*Lasers and Synergetics,* Vol. 19 of *Lecture Notes in Physics,* edited by R. Graham and A. Wunderlin (Springer-Verlag, Berlin, 1987).

[19]N. B. Abraham, P. Mandel, and L. M. Narducci, Prog. Opt. **25**, 1 (1987).

[20]J. Opt. Soc. Am. B, special issue, **5** (1988).

[21]J. Zorell, Opt. Commun. **38**, 127 (1981).

[22]L. M. Narducci, J. R. Tredicce, L. A. Lugiato, N. B. Abraham, and D. K. Bandy, Phys. Rev. A **33**, 1842 (1986).

[23]L. A. Lugiato, D. K. Bandy, L. M. Narducci, J. R. Tredicce, H. Sadiky, and N. B. Abraham, in *Optical Bistability III,* edited by H. M. Gibbs, P. Mandel, N. Peyghambarian, and S. D. Smith (Springer, Heidelberg, 1986), p. 293.

[24]L. A. Lugiato, L. M. Narducci, E. V. Eschenazi, D. K. Bandy, and N. B. Abraham, Phys. Rev. A **32**, 1563 (1986).

[25]L. A. Kotomtseva, N. A. Loiko, and A. M. Samson, J. Opt. Soc. Am. B **2**, 232 (1985).

[26]L. A. Kotomtseva, N. A. Loiko, and A. M. Samson, J. Appl. Spectrosc. **39**, 1245 (1983).

[27]L. W. Hillman, J. Krasinski, R. W. Boyd, and C. R. Stroud, Jr., Phys. Rev. Lett. **52**, 1605 (1984).

[28]C. R. Stroud, Jr., K. Koch, and S. Chakmakjian, in *Optical Instabilities,* edited by R. W. Boyd, M. G. Raymer, and L. M. Narducci (Cambridge University, Cambridge, England, 1986), p. 274.

[29]C. R. Stroud, Jr., K. Koch, S. Chakmakjian, and L. W. Hillman, Proc. Soc. Photo-Opt. Instrum. Eng. **667**, 48 (1986).

[30]N. M. Lawandy, R. S. Afzal, and W. S. Rabinovich, Phys. Rev. A **36**, 1759 (1987).

[31]L. W. Hillman, J. Krasinki, R. W. Boyd, and C. R. Stroud, Jr., Opt. Soc. Am. B **2**, 211 (1985).

[32]P. W. Milonni and M. L. Shih, J. Opt. Soc. Am. B **2**, 130 (1985); Opt. Commun. **53**, 133 (1985).

[33]L. W. Hillman and K. Koch, in *Optical Instabilities,* edited by R. W. Boyd, M. G. Raymer, and L. M. Narducci (Cambridge University, Cambridge, England, 1986), p. 256.

[34]Hong Fu and H. Haken, Phys. Rev. A **36**, 4802 (1987).

[35]Hong Fu and H. Haken, J. Opt. Soc. Am. B **5**, 899 (1988).

[36]Hong Fu and H. Haken, Phys. Rev. Lett. **60**, 2614 (1988).

[37]See, for example, L. W. Casperson, J. Opt. Soc. Am. B **5**, 958 (1988); **5**, 970 (1988), and references therein.

[38]H. Haken, *Laser Theory,* Vol. XXV/2c of *Encyclopedia of Physics,* 2nd ed. (Springer-Verlag, Berlin, 1984).

[39]H. Haken, *Light,* Vol. 2 of *Laser Light Dynamics* (North-Holland, Amsterdam, 1985).

[40]M. Sargent III, M. O. Scully, and W. E. Lamb, Jr., *Laser Physics* (Addison-Wesley, London, 1974).

[41]V. A. Yakubovich and V. M. Starzhinkii, *Linear Differential Equations with Periodic Coefficients* (Wiley, New York, 1975).

[42]H. C. Torrey, Phys. Rev. **76**, 1059 (1949).

[43]L. Allen and J. H. Eberly, *Optical Resonance and Two-Level Atoms* (Wiley Interscience, New York, 1975).